How to cite: *Angew. Chem. Int. Ed.* **2023**, *62*, e202306659
doi.org/10.1002/anie.202306659

C-H Activation

Preparative Scale Applications of C–H Activation in Medicinal Chemistry

*Rita de Jesus, Kerstin Hiesinger, and Manuel van Gemmeren**

Dedicated to Professor Rubén Martín.

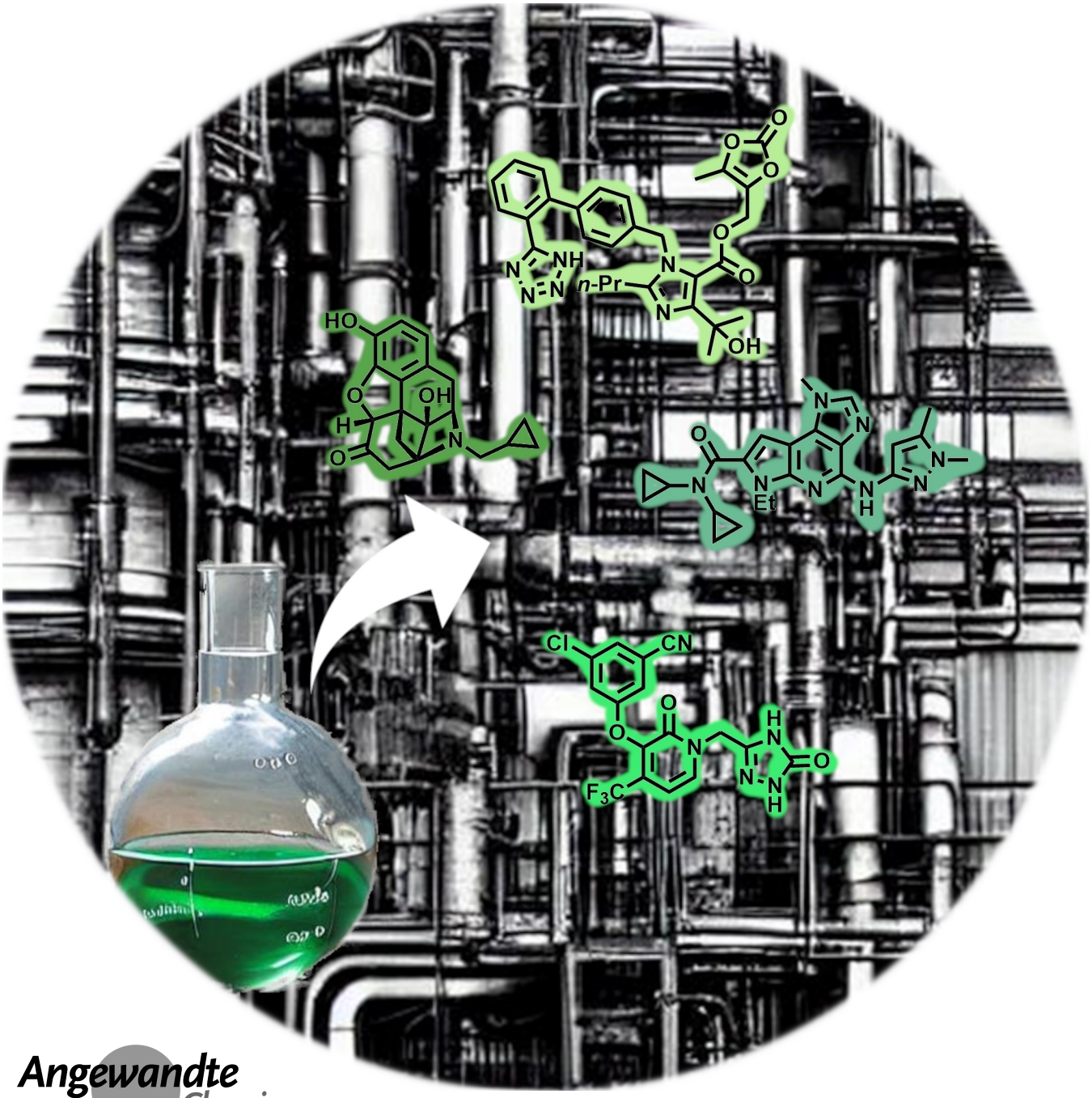

© 2023 The Authors. Angewandte Chemie International Edition published by Wiley-VCH GmbH

Abstract: C–H activation is an attractive methodology to increase molecular complexity without requiring substrate prefunctionalization. In contrast to well-established cross-coupling methods, C–H activation is less explored on large scales and its use in the production of pharmaceuticals faces substantial hurdles. However, the inherent advantages, such as shorter synthetic routes and simpler starting materials, motivate medicinal chemists and process chemists to overcome these challenges, and exploit C–H activation steps for the synthesis of pharmaceutically relevant compounds. In this review, we will cover examples of drugs/drug candidates where C–H activation has been implemented on a preparative synthetic scale (range between 355 mg and 130 kg). The optimization processes will be described, and each example will be examined in terms of its advantages and disadvantages, providing the reader with an in-depth understanding of the challenges and potential of C–H activation methodologies in the production of pharmaceuticals.

1. Introduction

The central role of synthetic organic chemistry in addressing societies key challenges of our time, such as healthcare, can easily pass by unnoticed. However, this discipline is indispensable, for example in the development of potent low-cost and thus widely available medicines. During drug development, medicinal and process chemists need to produce ever more complex organic compounds while facing time and cost pressure.[1] This leads to the requirement for robust and widely applicable synthetic methods, that enable the rapid generation of molecular complexity. Cross-couplings reactions, such as Suzuki–Miyaura coupling, are used extensively to form C–C or C–Het (heteroatom) bonds due to their reliability and broad substrate scope.[2] Nevertheless, these protocols have several inherent disadvantages such as the need for prefunctionalized substrates, causing additional synthetic steps and waste.[3] As a conceptual alternative, C–H activation does not require a prefunctionalization of substrates, in principle generating less waste and allowing step- and atom-economic synthesis from readily available starting materials.[4] In such methods, a transition metal catalyst is directly involved in the cleavage of a C–H bond forming a C–Metal bond through an inner-sphere mechanism (often a concerted metallation-deprotonation (CMD), but also through other mechanisms such as oxidative additions), followed by functionalization of the organometallic species. [5,6] This "shortcut", in comparison to traditional cross-couplings, serves material scientists,[7] has facilitated the total synthesis of natural products[8] and has enabled late-stage functionalizations (LSF) of compound libraries for medicinal chemistry programs (Scheme 1).[1b,6d,9]

Advances in catalyst and ligand design have enabled C–H activation not only on a bench-scale but also in multikilogram scale. Depending on the stage of drug development, different amounts of active compounds are required. During the drug discovery phase, the main goal is typically to obtain a few milligrams of compound for biological testing.[10] Thus, robust reactions with broad substrate scope rather than novel reactions that would require optimization, are preferred. At this stage, obtaining the target molecule quickly and in high purity is more important than high yields. Recent reviews have highlighted the increasing importance and utility of C–H activation in these early stages of medicinal chemistry research.[1b,9–10] As the compound moves from lead to candidate, higher quantities of compound are necessary for a wide range of studies. When a compound reaches clinical trials, kilogram amounts are often required, and in case the drug reaches the market, up to tons of material may be necessary.[11] Route optimization, which often includes the use of novel technology like flow chemistry or C–H activation, is usually undertaken at the end of drug development.

Factors such as safety, robustness, scalability, atom economy, cost and affording product in high purity are important criteria that enable the development of easy-to-scale-up methodologies.[3b,4b,12] Risk assessments should be performed in each step of the synthetic route, along with proper choice of reagents and solvents, to fulfil green chemistry criteria. The cost can be significantly lower if crystallizations and/or distillations are preferred over column chromatography, since the later requires large consumption of solvents and silica. Robustness and scalability to mitigate batch-to-batch fluctuation, and affording varying amounts when needed, respectively, are important factors

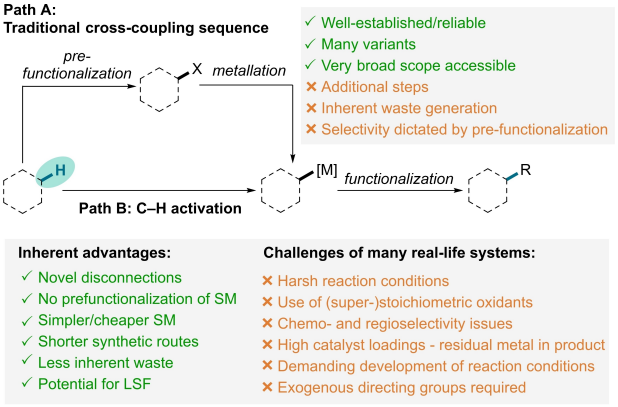

Scheme 1. Comparison between traditional cross coupling (Path A) and C–H activation (Path B). SM = starting material.

[*] R. de Jesus, Dr. K. Hiesinger, Prof. Dr. M. van Gemmeren
Otto-Diels-Institut für Organische Chemie, Christian-Albrechts-Universität zu Kiel
Otto-Hahn-Platz 4, 24118 Kiel (Germany)
E-mail: vangemmeren@oc.uni-kiel.de

© 2023 The Authors. Angewandte Chemie International Edition published by Wiley-VCH GmbH. This is an open access article under the terms of the Creative Commons Attribution Non-Commercial NoDerivs License, which permits use and distribution in any medium, provided the original work is properly cited, the use is non-commercial and no modifications or adaptations are made.

© 2023 The Authors. Angewandte Chemie International Edition published by Wiley-VCH GmbH

15213773, 2023, 45, Downloaded from https://onlinelibrary.wiley.com/doi/10.1002/anie.202306659 by Christian-Albrechts-Universitat, Wiley Online Library on [22/01/2025]. See the Terms and Conditions (https://onlinelibrary.wiley.com/terms-and-conditions) on Wiley Online Library for rules of use; OA articles are governed by the applicable Creative Commons License

that enable the development of easy-to-scale-up methodologies. These parameters can be addressed through C–H activation. Using cheap starting materials without prefunctionalization steps, lowers costs and enables the development of more atom economic synthetic routes. In addition, a deep mechanistic understanding of the synthetic methodology (e.g. impurity characterization) and detailed information about product variables (e.g. product isolation/purification) can lead to higher robustness. Taking these factors into account helps to accelerate the scale-up process, thereby saving time and money.[13] In addition, when planning to use C–H activation on scale, several other aspects need to be taken into consideration, some of which are inherent to the C–H activation process:[14] due to the stability of C–H bonds, substantial energy input/catalytic activity are required to induce this step, which can in turn also enable undesired processes. Thus, reactivity and chemoselectivity must be induced through catalyst control and a suitable selection of the reaction conditions. Additionally, the ubiquity of C–H bonds in organic molecules, renders the regioselective activation of a specific C–H bond challenging. To address that, a common strategy is the use of directing groups (DG):[15] by chelation to the catalyst, the substrate concentration close to the catalyst increases and enhances the reactivity (complex-induced proximity effect).[16] Selectivity is then determined by the position of the DG within the substrate. Importantly, the choice of DG (traceless, transient, or native) substantially influences the step- and atom-economy of the overall process. Additionally to the DG approach, nondirected methods have been developed with complementary reactivity and selectivity profiles.[17]

Further aspects arise, when C–H activation is to be applied on large scale:[3a] many C–H activation methods require high catalyst and/or ligand loadings, causing increased overall cost and waste production, as well as the possible presence of metal/ligands contaminants in the final product. The latter is of particular concern in the synthesis of active pharmaceutical ingredients (APIs) due to regulatory policies that must be fulfilled.[18] Various scavenging and recycling methodologies have emerged to address this matter. A further challenge resides in the external (stochiometric) oxidants, such as silver salts, that are commonly used in C–H activation methods to regenerate the active catalyst. However, some C–H activation methods are redox-neutral and general strategies exist that can be used to avoid the use of external oxidants for oxidative methods. Since methods without such oxidants are inherently more atom economic, designing scale up strategies based on a redox manifold that avoids the use of oxidant or use benign oxidation strategies, constitutes a notable strength of the respective methods.[19]

These challenges currently limit the use of C–H activation on large scale. However, the inherent ability of such methods to improve the efficiency of chemical processes, motivates research to unlock the full potential of this technology.

In this review, we will depict the role of C–H activation when moving to larger product quantities. Examples of pharmaceutically active compounds synthetized in preparatively relevant scales (from 355 mg up to 130 kg) that employ C–H activation in one or more key step of the synthetic route will be discussed. The discussion will be divided by the catalytically active metal (Rh, Ru, Ir, Pd). Within each section, examples are sorted by increasing scale of the C–H activation step. A detailed discussion of benefits and limitations will equip the reader with the knowledge

Rita de Jesus was born in Portugal. After receiving her B.Sc. degree in Applied Chemistry from Nova University of Lisbon, she pursued her M.Sc. in Bioorganic Chemistry in the same university. In 2021, she began her doctoral studies in the group of Prof. Manuel van Gemmeren at the University of Münster. One year later, the van Gemmeren lab moved to Kiel University, where she is continuing her studies in the field of nondirected C–H activation. She is interested in catalysis and natural product synthesis.

Kerstin Hiesinger studied chemistry at the Goethe University Frankfurt. She obtained her doctoral degree in medicinal chemistry (summa cum laude) from the laboratory of Prof. Eugen Proschak. After one year of postdoctoral studies in the same group, she joined Prof. van Gemmeren to perform postdoctoral studies on the synthesis of spirocyclic structures by C–H activation funded by the Walter Benjamin Programme. .

Manuel van Gemmeren, conducted his doctoral studies in the lab of Prof. Benjamin List (completed in 2014), followed by postdoctoral studies in the group of Prof. Rubén Martín. He led an independent research group at the University of Münster from 2016 to 2022, when he moved to Kiel University as professor for Organic Chemistry. Research in the van Gemmeren Lab focusses on the development of novel synthetic methods, typically based on C–H activation, that enable challenging transformations to proceed with catalyst-controlled reactivity and selectivity.

© 2023 The Authors. Angewandte Chemie International Edition published by Wiley-VCH GmbH

15213773, 2023, 45, Downloaded from https://onlinelibrary.wiley.com/doi/10.1002/anie.202306659 by Christian-Albrechts-Universitat, Wiley Online Library on [22/01/2025]. See the Terms and Conditions (https://onlinelibrary.wiley.com/terms-and-conditions) on Wiley Online Library for rules of use; OA articles are governed by the applicable Creative Commons License

required to judge the potential use of C–H activation methods in the production of pharmaceutically active compounds.[20]

2. Preparative Scale Applications of C–H Activation in Medicinal Chemistry

2.1. Rhodium

Due to its wide range of oxidation states (0 to +6) and broad functional group tolerance, rhodium has found many applications in C–H activation,[21] as demonstrated by the synthesis of naltrexone (**4**) reported in 2019.[22] **4** is used in the treatment of alcohol dependence and opioid abuse (Scheme 2A). Instead of relying on a natural product as starting material such as (−)-thebaine, Ellman et al. prepared precursor **1** from an achiral starting material in seven steps. The subsequent key step, an intramolecular Rh^{I}-catalyzed C–H alkenylation, was carried out on a 3.8 g scale to generate **2**, followed by in situ cyclization to a partially saturated isoquinoline **3** with the desired stereochemistry. Comparably high catalyst and high ligand loading (5 and 10 mol%, respectively) were used, without further optimization to reduce these loadings. The key C–H alkenylation step constitutes an application of a method previously reported by the same working group. In 2014, Ellman and co-workers reported the Rh-catalyzed synthesis of substituted tetrahydropyridines on a larger scale (Scheme 2B).[23] C–H activation occurred at the α,β-unsaturated imine **5**, followed by addition of the alkyne **6** to form an azatriene **7**, which undergoes electrocyclization to form **8**. Reduction with a hydride donor and acetic acid afforded tetrahydropyridines **9**. After optimization studies, the following conditions were developed: 1.5 equiv. alkyne, 0.5 mol% of the ligand 4-(diethylphosphino)-*N*,*N*-dimethylaniline and 0.25 mol% $[RhCl(coe)_2]_2$ (coe = cyclooctene) in toluene. However, due to the moisture sensitivity of the catalyst, the reactions had to be conducted in a glovebox. The authors thus decided to develop a second set of reaction conditions to enable benchtop use: an air stable catalyst $[RhCl(cod)]_2$ (cod = cyclooctadiene) was chosen for this purpose. To form the active catalyst, a 1 h induction period in toluene was required to promote dissociation of the strongly coordinating bidentate ligand. Higher temperature resulted in a drop in yield. To reach full conversion, the catalyst loading was increased to 1 mol%, enabling the reaction to be conducted outside a glovebox using standard inert atmosphere techniques. The applicability of both reaction conditions was demonstrated in four examples. 1 g scale reactions were performed and comparable yields were obtained with both catalysts. Terminal alkynes (in 1.2 equiv.) masked with a TMS group are suitable coupling partners for this reaction, but higher catalyst loading (0.5 mol% $[RhCl(coe)_2]_2$ and 1.5 mol% $[RhCl(cod)]_2$) are required. All reported yields were above 83 % after C–H activation, alkenylation, electrocyclization, and reduction. On a 20 g scale, the starting material was distilled to avoid catalyst poisoning and the desired molecule **8** was obtained in excellent yields, independently of the catalyst used (93 % yield with the air-stable catalyst, and in 95 % yield using the moisture-sensitive catalyst. Although $[RhCl(cod)]_2$ is used at a higher concentration compared to $[RhCl(coe)_2]_2$, the loading is still low, enabling an efficient and cost-effective synthesis.

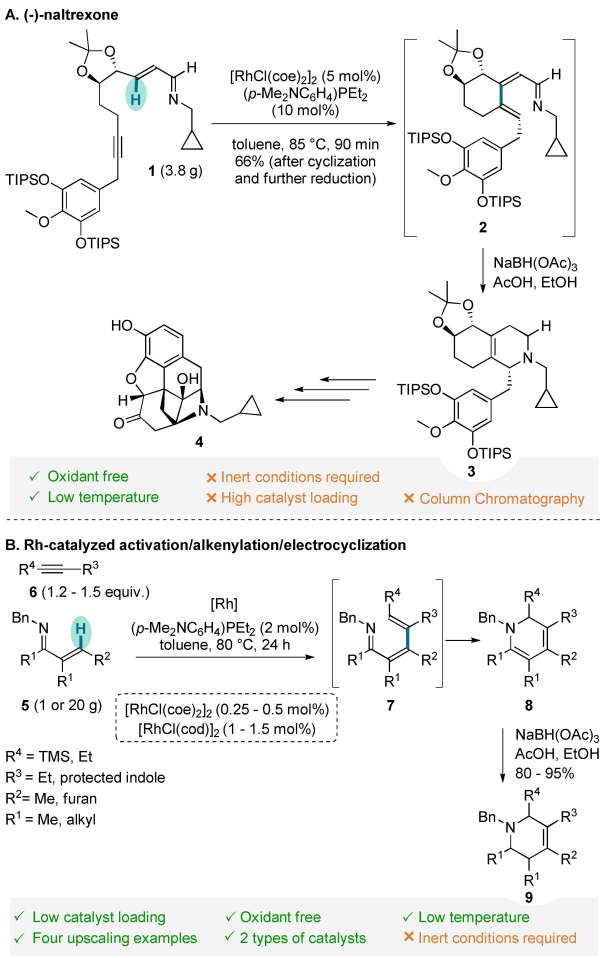

Scheme 2. A) Synthesis of (−)-naltrexone (**4**) via an intramolecular Rh-catalyzed C–H alkenylation. B) Rh-catalyzed C–H activation/alkenylation/electro-cyclization methodology.

2.2. Ruthenium

Ruthenium is a lower-cost transition metal, that can assume several oxidation states. As a result, this metal can engage in diverse mechanistic pathways, enabling orthogonal reactivity and selectivity in comparison to other metals. Ruthenium-catalyzed C–H arylation has become an efficient alternative to access biaryl scaffolds.[24] These moieties, commonly found in pharmaceuticals and agrochemicals,[1b] are highly valuable scaffolds in organic synthesis, as evidenced by the examples bellow.

The high demand for antihypertensive drugs requires the development of more efficient synthetic routes for angiotensin II receptor blockers (ARBs). In 2011, Seki reported a

© 2023 The Authors. Angewandte Chemie International Edition published by Wiley-VCH GmbH

15213773, 2023, 45, Downloaded from https://onlinelibrary.wiley.com/doi/10.1002/anie.202306659 by Christian-Albrechts-Universitat, Wiley Online Library on [22/01/2025]. See the Terms and Conditions (https://onlinelibrary.wiley.com/terms-and-conditions) on Wiley Online Library for rules of use; OA articles are governed by the applicable Creative Commons License

more sustainable approach to obtain ARBs[25] using a C–H arylation step (Scheme 3). To build the biphenyltetrazole core of ARBs, optimization studies showed that a combination of $RuCl_3 \cdot \times H_2O$ and PPh_3 (1:1.8 ratio with 1.3 mol% Ru-loading), proved to be a highly efficient catalytic system (Scheme 3A). The site-selectivity of the C–H activation step can be explained by the use of a native DG: chelation between the catalyst and the tetrazole moiety induces ortho-functionalization of the phenyl group. The presence of water in the catalyst plays an important role, since yields are drastically reduced when anhydrous ruthenium chloride is used, even when water is added separately. In a follow-up report, the author suggested that crystal water helps dissolving the catalyst,[26] while higher amounts of water (5 wt%) could cleave the acetoxy group of the coupling partner **11** and reduce conversion by generating unreactive low valent Ru species (Ru-black). Phosphine ligands, other than PPh_3, showed no improvement in yield. The choice of an appropriate protecting group (PG) on the tetrazole moiety is important due to potential catalyst poisoning from the free NH group. Bulky PGs, such as trityl, yielded no product, while methoxy-substituted benzyl PG proved beneficial. The use of diphenylmethyl instead of 2-methoxybenzyl resulted in a decrease in yield from 81 % to 7 %. Furthermore, the order in which reagents are added seems to play an important role in the reaction, and PPh_3 is required as both ligand and reducing agent. To test the optimized conditions, an intermediate of valsartan (**12a**) was synthesized using 1.3 mol% Ru catalyst and 1.8 mol% PPh_3 (0.5 mol% required to reduce the catalyst and 1.3 mol% ligand for the optimized metal-to-ligand ratio). The author reported a yield of 81 % (determined by HPLC) for the C–H activation step. Overall, valsartan (**13a**) was obtained in 55 % yield over 5 steps, starting from a protected phenyltetrazole **10a**. Scavenging methods, such as polymers coated with thiols, were tested and metals could be successfully recovered up to 98 % yield, improving the purity of the target molecule, atom economy and cost of the C–H activation step. In addition to valsartan, the author also synthesized losartan (**13b**, Scheme 3B). In contrast to the conditions optimized for 2-MeOBn-protected substrate **10b**, the author used a protocol adjusted to the 4-MeOBn group in this case, involving 10 mol% of another ruthenium source ($[RuCl_2(cod)]_n$) (10 mol%) and PPh_3 (20 mol%) to give product **12b** in 63 % yield after column chromatography.

Developing C–H activation methods using water, ligand-free conditions and at ambient atmosphere constitutes a substantial challenge. Towards this goal in 2018, Mehta and co-workers developed MCAT-53: a ruthenium catalyst synthesized by addition of sodium formate to Ru_2Cl_2(*p*-cymene), which promotes C–H arylations in water (Scheme 4A).[27] The catalyst is insensitive to moisture and is commercially available. The system chosen to test the catalyst was 3-trifluoro-2-phenyloxazoline (**14**) with aromatic bromides **15** and K_2CO_3. Under reflux conditions open to air, the authors observed high conversion, yield, and selectivity, isolating only the monoarylated product. Remarkably, despite the poor solubility of the various substrates in deionized water, the reaction proceeds smoothly and with good yield. After work-up, the aqueous layer can be reused if all reagents and half of the usual amount of catalyst are added again. However, no yield using only the recycled aqueous phase was reported. To demonstrate the applicability of their catalyst, the authors synthesized an intermediate **16** in the synthesis of anacetrapib (**17**), a drug indicated for the treatment of hypercholesterolemia. On a preparatively relevant scale, desired product **16** was isolated in 73 % yield after column chromatography.

In a related report published earlier (2011) by Ouellet et al., the C–H arylation was performed on a multikilogram scale to support the pharmacological evaluation of **17**, affording an almost quantitative yield of 96 % (Scheme 4B).[28] During optimization studies, the authors discovered that an impurity in the solvent NMP (γ-butyrolactone) improved the yields substantially. It was hypothesized that in the presence of base (K_3PO_4) and trace

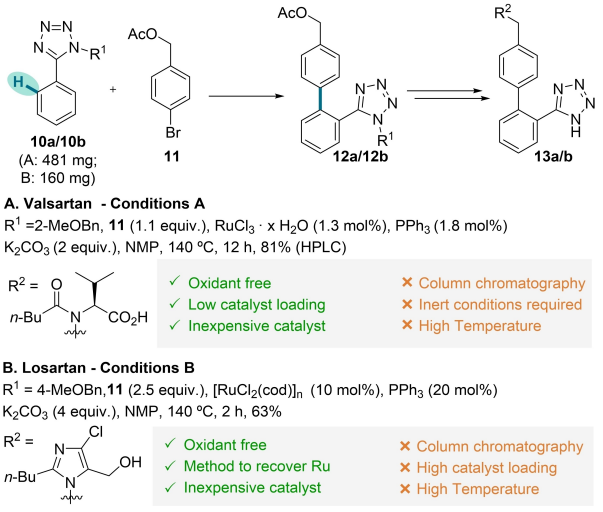

Scheme 3. A) Synthesis of valsartan (**13a**) via Ru-catalyzed C–H arylation B) Synthesis of losartan (**13b**) via Ru-catalyzed C–H arylation.

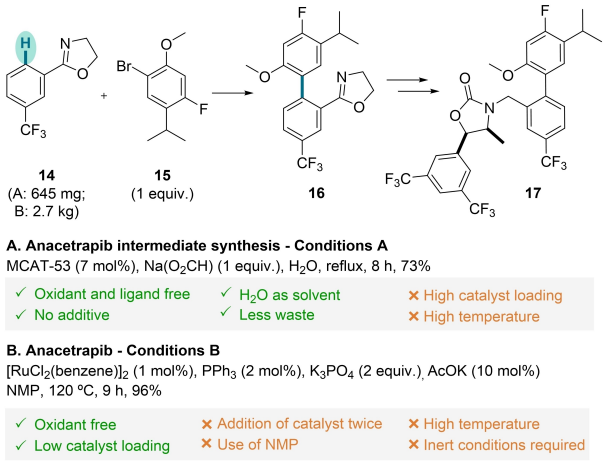

Scheme 4. Ru-catalyzed direct arylation A) using MCAT-53 in the synthesis of an anacetrapib intermediate **16**. B) in the synthesis of anacetrapib (**17**).

© 2023 The Authors. Angewandte Chemie International Edition published by Wiley-VCH GmbH

15213773, 2023, 45, Downloaded from https://onlinelibrary.wiley.com/doi/10.1002/anie.202306659 by Christian-Albrechts-Universitat, Wiley Online Library on [22/01/2025]. See the Terms and Conditions (https://onlinelibrary.wiley.com/terms-and-conditions) on Wiley Online Library for rules of use; OA articles are governed by the applicable Creative Commons License

amounts of water, the lactone hydrolysed and served as a carboxylate moiety, enhancing catalyst activity. To probe this hypothesis, the authors added catalytic amounts of KOAc and were able to reproduce the high yields in the absence of impurities. In their multikilogram synthesis, 1 mol% Ru catalyst and 2 mol% PPh_3 were used. When comparing both methods, Mehta et al. required higher catalyst loadings, but were able to avoid the use of a toxic solvent, ligands and inert conditions. The reduced waste production and lower overall costs render MCAT-53 an attractive option for scaling up purposes. Notably, the approval of this drug candidate was not pursued further by Merck & Co.[29]

Another approach for the efficient synthesis of ARBs was presented by Seki in 2012, in the synthesis of candesartan cilexetil (Scheme 5A).[30]

In this study, the challenge was to reduce the ruthenium loading and use a simple benzyl PG. When reducing the catalyst loading with the previously reported $RuCl_3 \cdot \times H_2O$/PPh_3 system, lower yields were observed. By switching to $[RuCl_2(p\text{-cymene})]_2$ in 0.32 mol% with 2 mol% of PPh_3, a conversion of 61 % was obtained. It should be noted that, when doubling the catalyst loading to 0.63 mol%, higher conversion and yield (86 % and 80 %, respectively) were achieved. Further modifications of the ligand or catalyst did not deliver any improvements. To demonstrate the applicability of this protocol, an intermediate of candesartan cilexetil **19** was synthetized on a 1 g scale from the benzylated tetrazole **18**, yielding the biaryl **19** in 80 % after workup and column chromatography, without a statement regarding the ratio of mono- vs. diarylation.

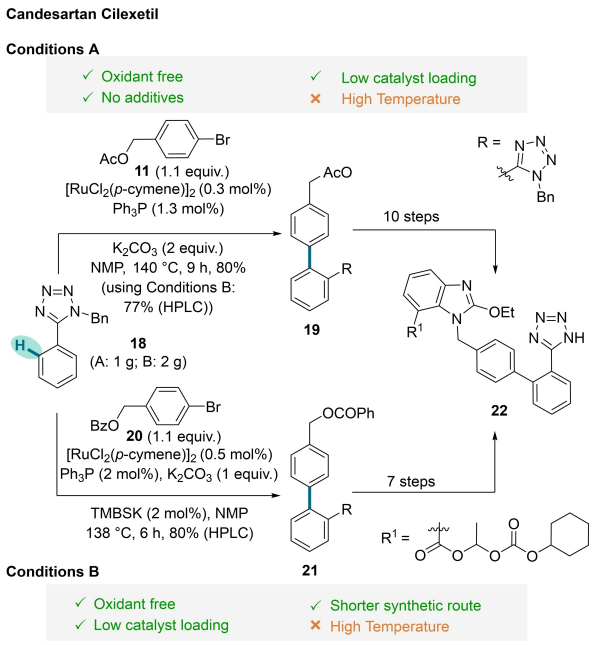

Scheme 5. A) Synthesis of candesartan cilexetil (**22**) via Ru-catalyzed direct arylation. B) Shorter synthetic route towards candesartan cilexetil (**22**).

Although optimization studies showed that a metal loading of 0.63 mol% (with 2 mol% ligand) would afford somewhat higher yields, a reduced metal loading of 0.3 mol% (with 1.3 mol% ligand) was used in the large-scale reaction. The reaction was performed in NMP at high temperature under inert conditions.

Two years later, the same author investigated potassium salts of various Brønstead acids as cocatalysts, while developing a shorter synthetic route to candesartan cilexetil (**22**, Scheme 5B). In the earlier report, acetylated aryl bromides **11** were used, while in this work benzoyl derivatives **20** were preferred, since they can be isolated by crystallization. Previously, Seki showed that potassium bis(2-ethylhexyl)phosphate induced a promising selectivity in C–H arylation.[31] The enhanced reactivity with this cocatalyst was explained by a ligand exchange and the assistance of the phosphate group in the CMD step. However, when bulky tetrazole derivatives **18** were used as substrates, such as those needed for the synthesis of ARBs, higher amounts of diarylated product were obtained. Potassium sulfonate derivatives were tested to increase reaction selectivity. Screening of several potassium additives showed that potassium 2,4,6-trimethylbenzenesulfonate (TMBSK) was the optimal additive, easier to handle than hygroscopic phosphate. Intermediates **19** and **21** were synthetized on a 2 g scale using 0.5 mol% $[RuCl_2(p\text{-cymene})]_2$, 2 mol% PPh_3, and 2 mol% sulfonate in NMP at 138 °C. After workup, the author analysed the filtrate by HPLC and determined a yield of 77 % for **19** (monoarylated) as well as 6.7 % of diarylated side product. Intermediate **21** was obtained in 80 % yield along with 10 % diarylated species determined by HPLC.[32] With the newly developed route, Seki was able to reduce the synthetic steps towards candesartan cilexetil (**22**) from 10 to 7, concomitantly improving the atom economy. The biphenyl motif was generated by C–H activation, which showed a higher atom efficiency than the cross-coupling reaction employed in the initially reported route (61 % vs. 34 %).

When comparing both C–H arylation protocols, yields are similar, but the generation of intermediate **21** requires a higher metal and ligand loading, as well as an additive, rendering the protocol towards intermediate **19** (conditions A) more atom economical, an advantage that is counterbalanced by the reduced number of subsequent steps when using conditions B.

Seki's work on the C–H activation of tetrazole-containing biaryls may pave the way for large-scale C–H activation-based synthesis of ARBs. In addition to lorsartan (**13b**), valsartan (**13a**), and candesartan cilexetil (**22**), the author also published a procedure for the synthesis of olmesartan medoxomil (**25**, Scheme 6).[33]

In contrast to earlier studies, the use of a benzyl PG resulted in poor yields and in the formation of by-products in the final cleavage step. Therefore, the author switched to the bulkier 2,4-dimethoxybenzyl (DMB) PG on the tetrazole moiety **23**, which can be cleaved with TFA in dichloromethane in near quantitative yield. In contrast to the results with a benzyl PG, the sterically more demanding group gave exclusively monoarylated product **24** upon C–H activation

© 2023 The Authors. Angewandte Chemie International Edition published by Wiley-VCH GmbH

15213773, 2023, 45, Downloaded from https://onlinelibrary.wiley.com/doi/10.1002/anie.202306659 by Christian-Albrechts-Universitat, Wiley Online Library on [22/01/2025]. See the Terms and Conditions (https://onlinelibrary.wiley.com/terms-and-conditions) on Wiley Online Library for rules of use; OA articles are governed by the applicable Creative Commons License

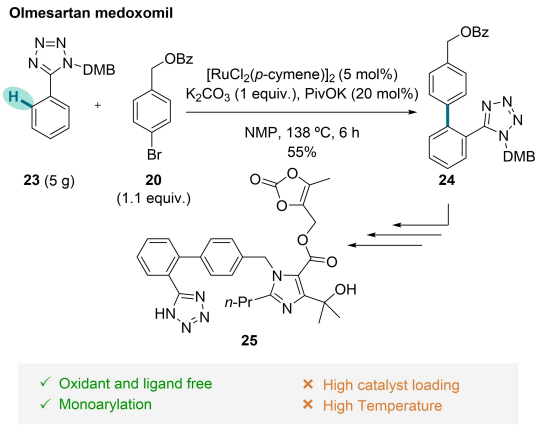

Scheme 6. Direct C–H arylation in the synthesis of olmesartan medoxomil (**25**).

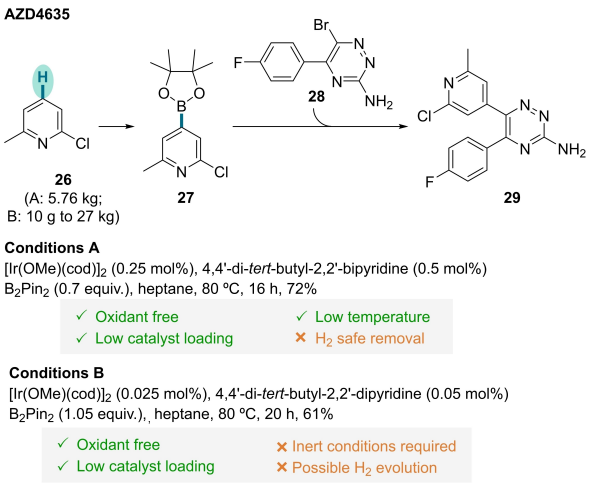

Scheme 7. A) Synthesis of AZD4635 (**29**) via Ir-catalyzed direct borylation. B) Previous C–H borylation protocol for the synthesis of AZD4635 (**29**).

with **20** as coupling partner. Biaryl product **24** was synthetized giving a moderate yield of 55 % after column chromatography on a 5 g scale when using 5 mol% of $[RuCl_2(p\text{-cymene})]_2$ as catalyst, and potassium pivalate as additive.

Seki's work shows that despite the similar core structure of ARBs, extensive fine-tuning is required for C–H activation. In each case, a different PG, additives, and catalysts can be required for an optimal reaction outcome.[34] Ultimately, the main task for the medicinal chemistry/process chemistry intersection will be fine-tuning to achieve robust, high-yielding, and highly selective C–H activation methods.

2.3. Iridium

Organoboron compounds are versatile synthetic building blocks for the formation of C–C, C–O, C–N, and C–X bonds. An elegant route to access these compounds is through C–H activation using iridium as transition metal catalyst.[18,35] The Ir-catalyzed borylation of arenes is in general sterically controlled and does not require directing groups.[35a] In heteroarenes, regioselectivity varies and is controlled by a combination of steric and electronic effects.[36] Pyridines, for example, are borylated in β- or γ-position to the basic nitrogen. Due to the mild reaction conditions, high selectivity and low catalyst loading, iridium-assisted borylation was embedded in the synthetic pathway to generate AZD4635 (**29**). API **29**, an antagonist of the adenosine A2 A receptor, is in clinical trials as monotherapy or in combination with other drugs for the treatment of solid tumors.[37] Klauber et al. reported a multikilogram-scale synthesis of AZD4635 (**29**) in 2018 (Scheme 7A),[38] wherein a pinacol boronate ester **27** was required to perform a Suzuki–Miyaura cross-coupling.

C–H activation was carried out using the commercially available starting material chloro-6-methylpyridine (**26**), with (1,5-cyclooctadiene)(methoxy)-iridium(I) dimer $[Ir(OMe)(cod)]_2$ as catalyst and 4,4′-di-*tert*-butyl-2,2′-bipyridine (dtbpy) as ligand. Bis(pinacolato)diborone (B_2pin_2) served as the borylating agent, which could be used in 0.7 equiv., since 4,4,5,5-tetramethyl-1,3,2-dioxaborolane (HBpin) formed as by-product in the borylation can also serve as a borylating agent. To form the active catalyst, precatalyst, ligand, and B_2pin_2 were preheated to 50 °C in heptane for 0.5–3 h, before pyridine substrate **26** was added. The product was isolated in 72 % yield after crystallization. One challenge for large-scale synthesis was the stoichiometric formation of HBpin as by-product, which reacts with moisture, water, or alcohols to produce hydrogen gas. Notably, hydrogen is also formed as by-product, when HBpin acts as borylating reagent in the desired C–H borylation. Therefore, inert conditions were required and, to ensure safe hydrogen removal, the venting capacity of the reactor was checked. Various precautions such as the use of non-conductive solvents, low oxygen levels, and grounding of containers and plugs were also implemented. Afterwards, to efficiently remove metal traces, the authors relied on a well-designed crystallization, without the use of scavenging techniques. In a follow up study from 2022, Meadows and co-workers further investigated hydrogen evolution in the borylation reaction for the synthesis of the same API (**29**, Scheme 7B).[39] The reaction was also conducted in heptane with iridium as the catalyst, and B_2pin_2 as the borylation agent. In a high-throughput experimental screening, different catalysts and various bipyridine- and phenanthroline-based ligands were tested. As in the previous work, dtbpy was selected as ligand due to its availability, acceptable cost, and good performance. The volume of heptane could be reduced by 40 % without compromising the reaction efficiency. To further optimize the reaction conditions, the catalyst loading and the equiv. of B_2pin_2 were investigated. To avoid the generation of hydrogen, 1 equiv. of B_2pin_2 was used. Varying the catalyst loading of $[Ir(OMe)(cod)]_2$ between 0.025 mol% and 0.0025 mol% significantly decreased the yield. Although 0.0125 mol% iridium catalyst gave a 97 % conversion after 20 hours, a higher loading was

© 2023 The Authors. Angewandte Chemie International Edition published by Wiley-VCH GmbH

15213773, 2023, 45, Downloaded from https://onlinelibrary.wiley.com/doi/10.1002/anie.202306659 by Christian-Albrechts-Universitat, Wiley Online Library on [22/01/2025]. See the Terms and Conditions (https://onlinelibrary.wiley.com/terms-and-conditions) on Wiley Online Library for rules of use; OA articles are governed by the applicable Creative Commons License

used because of concerns about catalyst deactivation if the experiments were performed outside the glovebox. The reaction is quite sensitive to oxygen, so purging with nitrogen and monitoring of oxygen levels were required. The final conditions were 0.025 mol%$[Ir(OMe)(cod)]_2$, 0.05 mol% dtbpy, and 1 equiv. B_2pin_2 in heptane, yielding a conversion of over 98%. The HBpin-containing waste was kept under inert conditions and treated with anhydrous ethanol to quench HBpin. The product of C–H activation **27** was isolated by crystallization, and residual HBPin was washed out with heptane. With the safer protocol developed, the authors could synthesize over 70 kg of **27** in two batches (batch 1 with 27 kg and batch 2 with 26.1 kg of **26**). Despite the dangers associated with HBpin as side product, both approaches successfully synthesized C–H borylated product in high yields. The use of very low catalyst loadings, shows that catalyst fine-tuning is key to run C–H activation under mild conditions on a large scale.

Although iridium is expensive, it is widely used in industry due to low catalyst loadings and the lower efficiency of alternative approaches. This is reflected in the synthesis of GSK8175 (**32**), a boron-containing RNA polymerase (namely NS5B) inhibitor that is in clinical trials for the treatment of hepatitis C (Scheme 8).[40]

For the construction of a C–N bond via Cham-Lam coupling, Kowalski, Leitch, and co-workers synthetized the organoboron reagent **31** using an Ir-catalyzed C–H activation step (Scheme 8A). In the first borylation experiments, methods described in the literature were used: 1 mol% $[Ir(OMe)(cod)]_2$, 2 mol% dtbpy, B_2pin_2 in heptane/TBME mixture. Optimization studies to reach scalability replaced the catalyst system for the widely available $[Ir(cod)Cl]_2$, and 2,2′-bipyridine (bipy) as ligand. In addition, based on literature reports, preactivation of the metal/ligand mixture in presence of B_2pin_2 (85 °C for 30 min under inert conditions) was necessary to generate the active catalyst. At this temperature, co-solvents such as TBME were no longer required and were even shown to be detrimental to the reaction outcome. The morphology of the catalyst plays an important role, and finely powdered $[Ir(cod)Cl]_2$ resulted in a more active catalyst than coarse-crystalline catalyst, which the authors explained by faster dissolving of the fine powder in heptane. With these observations, the authors were able to reduce the loadings to 0.4 mol% of $[Ir(cod)Cl]_2$ and 0.8 mol% of dtbpy. On a 228 g scale, **31** was isolated in 91% yield after crystallization. In a synthesis reported one year later by Peat et al.,[41] the loading was even lower (Scheme 8B): using 0.2 mol% $[Ir(cod)Cl]_2$ and 0.4 mol% of ligand 5,5′-di-*tert*-butyl-2,2-bipyridine at 56 °C for 21 h, 88% of the borylated product **31** was obtained. The exact scale was not reported, but in the end, the authors produced more than 3 kg of GSK8175 (**32**) in less than 10 months, after the initial synthesis in their medicinal chemistry laboratories.

The synthesis of AZD4573 (**35**) demonstrated the superiority of C–H activation/borylation over prefunctionalization and palladium-catalyzed borylation on a large scale (Scheme 9).[42]

In order to rapidly provide AZD4573 (**35**), an oncology drug candidate, in sufficient quantities for preclinical and clinical studies, several steps of the medicinal chemistry route had to be modified. One of the changes was the borylation step. The original Pd-catalyzed method afforded only moderate yields (about 50%), so optimization was needed to improve yields and atom efficiency. In the second-generation route, lithium-halogen exchange, followed by borylation was investigated. Although high yields (92%) and easy workup were achieved, cryogenic conditions raised concerns for further scale-up processes. To avoid prefunctionalization, C–H activation/borylation was investigated with heterocycle **33**. Borylation of the substituted pyrazole occurred in β-position to the nitrogen atoms as independently reported by Hartwig[36] and Smith, Maleczka, and Krska.[43] An initial screening was performed in the glovebox with 5 mol% $[Ir(OMe)(cod)]_2$, inspired by reports of large-scale Ir-catalyzed borylations. Ligand screening revealed 3,4,7,8-tetramethylphenanthroline (tmphen) as a suitable ligand in polar solvents. Notably, dtbpy performed comparably as a ligand, but Karlsson and co-workers pursued further optimization using tmphen. Variations of

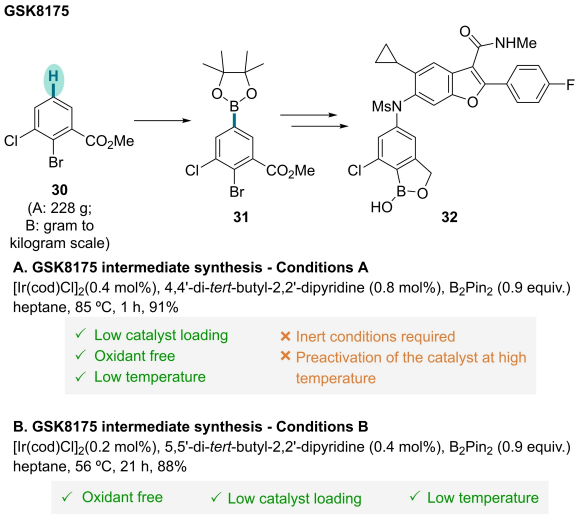

Scheme 8. A) Synthesis of GSK8175 (**32**) via Ir-catalyzed direct borylation. B) Follow up C–H borylation protocol for the synthesis of GSK8175 (**32**).

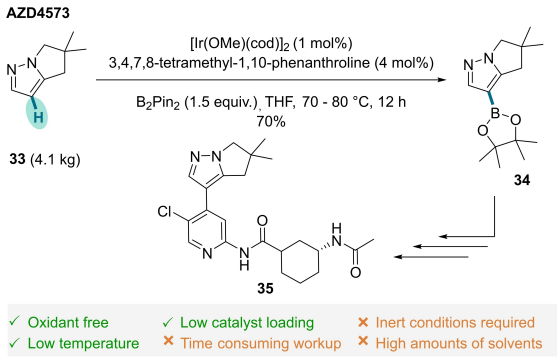

Scheme 9. Synthesis of AZD4573 (**35**) via Ir-catalyzed direct borylation.

© 2023 The Authors. Angewandte Chemie International Edition published by Wiley-VCH GmbH

15213773, 2023, 45, Downloaded from https://onlinelibrary.wiley.com/doi/10.1002/anie.202306659 by Christian-Albrechts-Universitat, Wiley Online Library on [22/01/2025]. See the Terms and Conditions (https://onlinelibrary.wiley.com/terms-and-conditions) on Wiley Online Library for rules of use; OA articles are governed by the applicable Creative Commons License

catalyst and ligand loading as well as the solvent were studied and nearly all screening entries gave complete conversion within 23 hours at temperatures between 60 and 80 °C. The authors were able to lower the catalyst loading to 1 mol% and the ligand loading to 4 mol% with 1.5 equiv. of B_2pin_2 in THF. Complete conversion was observed by UHPLC within 3 hours. To transfer the method from the glovebox to the reactor, the oxygen level was controlled (headspace was kept below 5000 ppm oxygen) through several nitrogen-vacuum cycles. In order to obtain the borylated product **34** in high purity, a laborious workup and crystallization process was developed: activated carbon treatment along with filtration to remove impurities; solvent exchange (from THF to methanol and water), followed by heating and cooling steps for crystallization. Finally, the authors isolated 5.6 kg (70 % yield) of the pure borylated product **34**. The major drawback of this route lies in the purification that is time intensive and consume large volumes of organic solvents. However, compared with the method relying on bromination followed by lithium-halogen exchange and borylation, the sustainability was nevertheless improved significantly.

In 2021, Ironmonger and Wheelhouse et al.[44] developed a new pathway for accessing nemiralisib (**38**), which was studied as a treatment option for chronic obstructive pulmonary disease (Scheme 10).[45] To generate sufficient amounts of the API for safety studies and Phase I clinical trials, 5 kg of nemiralisib (**38**) were synthesized. Two C–H activation steps were used as part of the route. In this section, the Ir-catalyzed reaction is highlighted, while the preceding Pd-catalyzed reaction will be discussed in the next section (*cf.* Scheme 24). Iridium-assisted borylation is well-established, however, heteroaryl C–H bond borylation has been studied to a lower extent. In this particular case, the authors had concerns about borylation occurring on both heteroaryl rings. Using $[Ir(OMe)(cod)]_2$, 5,5′-di-*tert*-butyl-2,2-bipyridine as ligand and 1.2 equiv. B_2pin_2, a mixture of regioisomeric monoborylated species was detected as minor components, alongside diborylated species as main products. Further screening with B_2pin_2 or HBpin in THF or 2-MeTHF revealed that HBpin in THF gave the highest amounts of diborylation (88 % as determined by HPLC). Instead of optimizing the reaction towards selective mono-borylation, the authors developed an elegant way of selectively cleaving the undesired C–B bond. Screening of aqueous acids and bases failed to cleave the labile oxazole C–B bond, while heating the diborated species with isopropanol selectively cleaved the undesired C–B bond, while the indazole C–B bond remained intact. While establishing this route, the authors saw an opportunity to reduce the synthetic steps towards nemiralisib (**38**) and adjusted the substrate structure for the borylation step. Substantial additional optimization was required when changing to substrate **36** and the ligand was changed to 3,4,7,8-tetramethyl-1-10-pehanthroline. Through this reoptimization the formation of product **37** was improved (60 %), with almost no monoborylations occurring at other positions. During these optimization studies, the authors also demonstrated that a PG of the indazole moiety is necessary, and no product formation was observed with the indazole free N–H. Within 4 h in THF, consumption of the starting material **36** was observed with 1 mol% $[Ir(OMe)(cod)]_2$, 2 mol% tmphen and 3 equiv. HBpin. Reduction of the catalyst loading to 0.5 mol% was possible, but residues of amide in the starting material inhibited the reaction. To achieve more robustness, 1 mol% dimeric catalyst and 5 mol% tmphen were used. Under these conditions the reaction was performed on a 54 kg scale, giving product **37** in 83 % yield after crystallization.

Doravirine (**41**), which is used to treat HIV infection, was synthesized on a kilogram scale by Campeau et al. to support clinical studies (Scheme 11).[46] When performing the reaction on a milligram-scale, impurities in the API (polymethylation and polycyanation) where encountered, which could only be purified by preparative HPLC. To develop a robust and scalable route, a new pathway was chosen. In the first step, a dihalogenated benzene derivative **39** was selectively borylated via C–H activation in the meta position. In the initial experiments, dtbpy was used as ligand and $[Ir(OMe)(cod)]_2$ as catalyst. However, the high cost and long lead times forced the authors to look for alternative

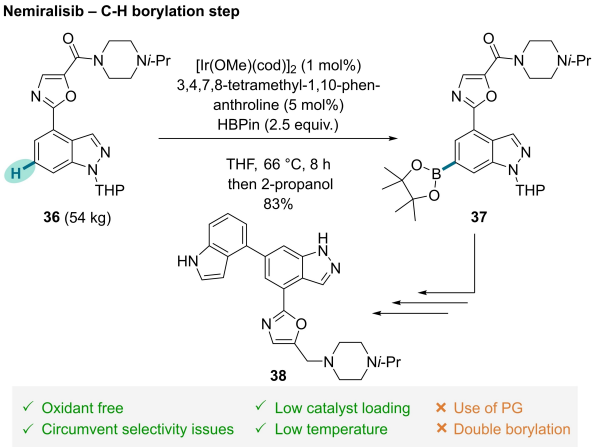

Scheme 10. Ir-catalyzed C–H borylation step in the synthesis of nemiralisib (**38**).

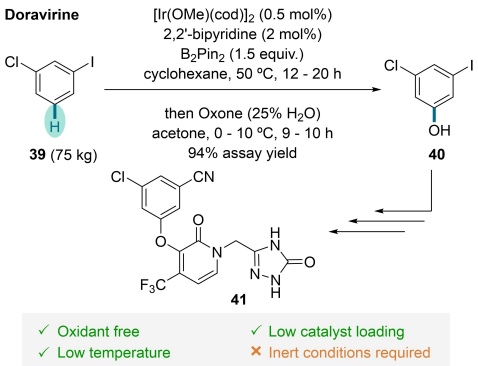

Scheme 11. Synthesis of doravirine (**41**) via Ir-catalyzed direct borylation.

© 2023 The Authors. Angewandte Chemie International Edition published by Wiley-VCH GmbH

15213773, 2023, 45, Downloaded from https://onlinelibrary.wiley.com/doi/10.1002/anie.202306659 by Christian-Albrechts-Universitat, Wiley Online Library on [22/01/2025]. See the Terms and Conditions (https://onlinelibrary.wiley.com/terms-and-conditions) on Wiley Online Library for rules of use; OA articles are governed by the applicable Creative Commons License

ligands. Pleasingly, simple 2,2′-bipyridine met their requirements. During optimization, the loading of the catalyst was reduced from 1.5–3 mol% to 0.8–1 mol%. The reaction was carried out in cyclohexane and the borylation product was directly further converted to the phenol **40** by oxidation with oxone. Borylation was carried out in a 75 kg scale under inert conditions at low temperature with 0.5 mol% catalyst, 2 mol% ligand, and 1.5 eqiuv. B_2pin_2. 75.3 kg of the oxidized product **40** were obtained over two steps. The use of a simple ligand as well as low catalyst and ligand loadings are compelling features of this synthesis.

2.4. Palladium

From traditional cross-couplings to C–H activation, palladium is the most widely employed transition metal. The development of robust reactions such as arylation, alkynylation, and olefination where only possible due to well-studied catalytic cycles, proving the general synthetic utility of palladium catalysts.[47] In 2005, Fagnou et al. reported a Pd-catalyzed direct arylation of pyridine *N*-oxides.[48] The concept was further extended in 2012 by Zhao, Wang and co-workers in the development of a Pd-catalyzed direct arylation of imidazolone *N*-oxides **42**.[49] Before the application of this method for the synthesis of a pharmacologically active compound (Scheme 12), reaction optimization was performed. Using imidazolone *N*-oxide as initial substrate and applying similar conditions as reported by Fagnou and co-workers - $Pd(OAc)_2$ (5 mol%), PPh_3 (15 mol%), and K_2CO_3 in toluene - selective arylation in the 4-position was achieved, independently of the steric hindrance in the 2-position. Solvent exchange to dioxane slightly improved the yields. Protection of the free N–H group with 2,4-dimethoxybenzyl afforded higher yields and lower levels of deprotection, compared to the use of Boc protected starting material. Aryl bromides, such as **43**, were chosen as coupling partners due to increased selectivities in comparison to aryl chloride/iodides. To prove the synthetic utility of the protocol, the C–H arylation step was implemented on a preparatively useful scale (355 mg) within a linear synthesis of GSK2137305 (**45**). When these studies were conducted in 2012 and until 2020, this compound was considered a potential treatment for neuropsychiatric disorders. The C–H arylated product **44** was obtained in 64 % yield after column chromatography. The purification method is one of the drawbacks of the method since more waste is generated. However, the absence of chemical oxidants and use of imidazolone *N*-oxides as an alternative starting point towards 4-aryl imidazolone *N*-oxides, are strengths of this protocol.

As part of a medicinal chemistry program, McClure and co-workers initially relied on a Suzuki–Miyaura coupling with a commercially available but expensive boronic acid, in order to obtain 5-aryl-furfural derivatives **48**. Since the reagent cost would hamper scaling up this process, in 2001, the authors reported a Pd-catalyzed C–H arylation of furfural (Scheme 13A).[50]

Following a "statistically driven approach" using as coupling partner 4-iodo-chlorobenzene (**47**), several parameters were screened to detect synergies and accelerate the reaction optimization. To avoid/minimize homocoupling as side reaction and increase conversion, the authors describe that the best strategy is to add the arylating reagent **47** via syringe pump (over 10 h) to the furfural (**46**). The optimal

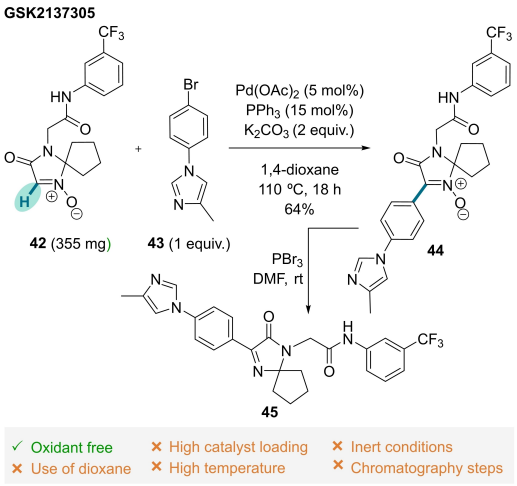

Scheme 12. Synthesis of GSK2137305 (**45**) via Pd-catalyzed direct arylation.

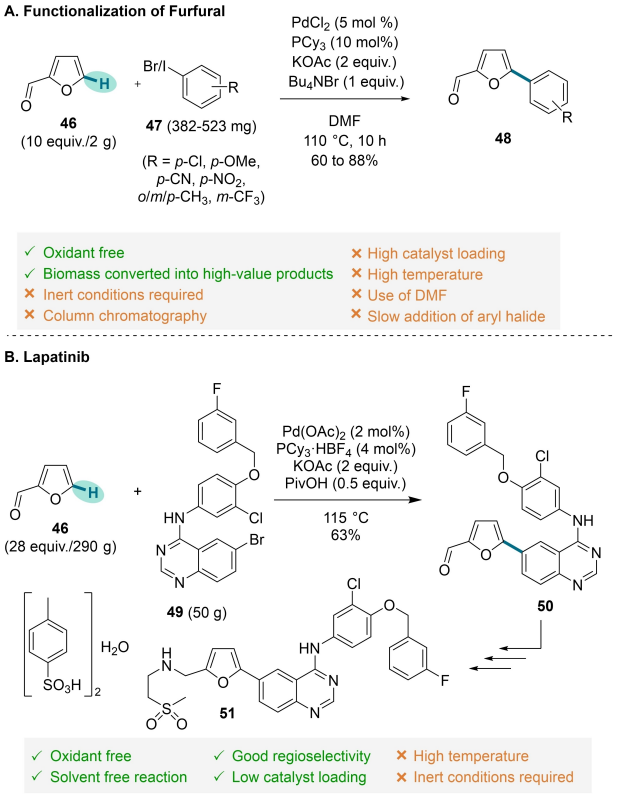

Scheme 13. A) Furfural (**46**) functionalization via Pd-catalyzed direct arylation. B) Synthesis of lapatinib (**51**) via Pd-catalyzed direct arylation of furfural (**46**).

© 2023 The Authors. Angewandte Chemie International Edition published by Wiley-VCH GmbH

15213773, 2023, 45, Downloaded from https://onlinelibrary.wiley.com/doi/10.1002/anie.202306659 by Christian-Albrechts-Universitat, Wiley Online Library on [22/01/2025]. See the Terms and Conditions (https://onlinelibrary.wiley.com/terms-and-conditions) on Wiley Online Library for rules of use; OA articles are governed by the applicable Creative Commons License

conditions involved KOAc as base (reduced side product formation in comparison to *N*,*N*-diisopropylethylamine), $PdCl_2$ as catalyst (higher conversions relative to $Pd(OAc)_2$), and Cy_3P as ligand (to expand the reaction scope although $PdCl_2$ in DMF showed similar results with or without ligand). Within a range of 382–523 mg scale, the reaction was tested using several substrates, affording products **48** in 60 to 88 % isolated yield. The authors mention two possible mechanistic pathways: either a traditional Heck-type mechanism or through a "divinyl Pd^{II} intermediate". The latter (C–H activation pathway) can be considered more likely, since no de-aromatization is required and due to the analogy to related reactions described in literature.[51] Additionally, in a Heck-type pathway, the β-hydride elimination would be disfavored by the necessity to adopt a syn-periplanar conformation. The described approach is limited by the use of column chromatography and high temperature. However, the direct functionalization of commodity chemicals, including a renewable feedstock starting material, bears large application potential.

The C–H arylation protocol described above was employed as part of a novel synthetic route towards lapatinib (**51**, Scheme 13B).[52] Lapatinib (**51**) is a drug used for the treatment of advanced or metastatic breast cancer, and analogous to the work by McClure and co-workers, the Suzuki–Miyaura coupling step had to be replaced. The generation of hazardous wastes in addition to the multistep synthesis of the boronic acid, were underlying reasons that contributed to the use of C–H activation. Conditions reported by McClure et al.[50] and Doucet et al.[53] afforded a complex mixture of side products and product, and higher conversions were only obtained when furfural (**46**) was used in excess. In contrast, modification of the Fagnou protocol afforded full conversion in 2–3 h using furfural in excess (solvent and reactant).[54] During reaction optimization, $Pd(OAc)_2$ proved to be the optimal Pd-source; the choice of ligand strongly influenced the reaction selectivity and reaction rate, the best results being obtained with $Cy_3P{\cdot}HBF_4$. PivOH as an additive in the range of 0.3–0.5 equiv. proved to be the most efficient additive; as base KOAc gave a slower reaction compared to K_2CO_3, but no formation of bis-furfural was detected when using KOAc. Under the optimized conditions, using 50 g of coupling partner **49**, C–H arylation was performed. The purification involved the addition of acetone, filtration, and addition of water, followed by filtration in a complex series of heating and cooling steps. Intermediate **50** was isolated in 63 % yield and could be converted further into lapatinib (**51**). Substituting the Suzuki–Miyaura coupling with a modern C–H activation methodology, enabled an overall more atom efficient and shorter synthetic route towards this drug.

The small electronic and steric differences among C–H bonds in heterocycles, can be a challenge in the development of highly regioselective C–H functionalization methods.[55] In the commercial route of celecoxib (**55**), a non-steroidal anti-inflammatory drug, a mixture of pyrazole regioisomers was obtained, undermining subsequent purification.[56] Therefore, in 2011, Gaulier et al. reported a linear synthetic route of celecoxib (**55**) based on a regioselective Pd-catalyzed C-5 arylation methodology (Scheme 14), thereby expanding the scope of C–H arylations in 1,3-disubstituted pyrazoles.[57] Using almost stoichiometric metal and ligand loading, the C–H activation step was performed on a preparative scale using **52** and **53**. The arylated product **54** was obtained in 66 % yield after column chromatography (containing less than 5 % of C4/C5 di-arylated product). The very high amount of catalyst required constitute a key drawback of this protocol, limiting its application in larger scale synthesis. The improved regioselectivity can be rationalized by a CMD pathway enabled by the pivalate ligand, however no in-dept mechanistic studies were performed.

In the originally patented synthesis of the anxiety mediator ($GABA_A$ $\alpha_{2,3}$-selective agonist) **59** (Scheme 15A),[58] the C–C bond formation was achieved through a Suzuki–Miyaura coupling. However, the multistep synthesis of the required aryl boronic acid called for an alternative disconnection approach. In 2005, Jensen et al. developed a scalable synthetic route towards **59**, in order to supply drug trials using two palladium-catalyzed reactions: an apparent "Heck-type reaction" and a Suzuki–Miyaura coupling as final stages of the synthesis (Scheme 15A).[59] Analogously to celecoxib (**49**), a Heck-type mechanism seems unlikely. A more reasonable pathway involves a C–H activation by the Pd^{II} species on the 3-position of substrate **56**, forming an aryl(heteroaryl)palladium(II) intermediate, which then forms product **58** through reductive elimination. Regioselective C-3 arylation can be explained by the increased reactivity of this position towards C–H activation. Optimization studies showed that K_2CO_3 and DMF could be used as alternatives to Cs_2CO_3 and 1,4-dioxane, respectively. The optimal ligand was PPh_3 without further screening details. After reaction optimization, and using **57** as coupling partner, a 10.6 g C–H arylation afforded product **58** in 88 % yield, using an extractive workup as purification method. The contamination of products with metal and ligands should be as low as possible, especially in API synthesis. Thus, "ligand-less" systems and low catalyst loadings are highly desirable, not only for cost-reasons. Based on the fact that the acidic aqueous solution from the Suzuki–Miyaura-

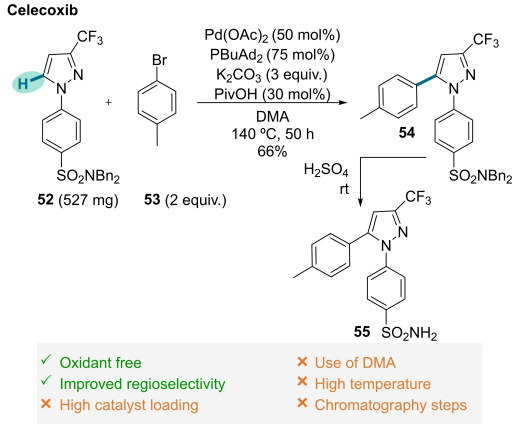

Scheme 14. Synthesis of celecoxib (**55**) via Pd-catalyzed direct arylation.

© 2023 The Authors. Angewandte Chemie International Edition published by Wiley-VCH GmbH

15213773, 2023, 45, Downloaded from https://onlinelibrary.wiley.com/doi/10.1002/anie.202306659 by Christian-Albrechts-Universitat, Wiley Online Library on [22/01/2025]. See the Terms and Conditions (https://onlinelibrary.wiley.com/terms-and-conditions) on Wiley Online Library for rules of use; OA articles are governed by the applicable Creative Commons License

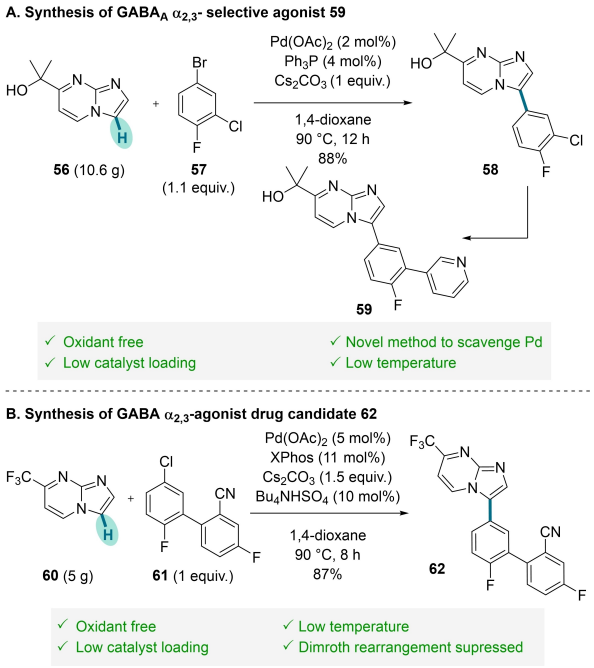

Scheme 15. Pd-catalyzed arylation in the A) synthesis of GABA$_A$ $\alpha_{2,3}$-selective agonist **59** and B) GABA $\alpha_{2,3}$- agonist drug candidate **62**.

coupling was yellow, the authors hypothesized that Pd^{II} was present in solution. Therefore, borane-trimethylamine complex was added to solution in an attempt to reduce the metal to Pd^0. Gratifyingly a black precipitate was obtained, which after filtration, basic/acid treatment, Darco-G60 filtration and crystallization, yielded the final molecule **59** with less than 3 ppm Pd content. Considering the presence of several heteroatoms in the final molecule and the use of two Pd-catalyzed reactions, an efficient method for metal removal was developed. Direct arylation proved to be a more atom economic approach in comparison to the initial Suzuki–Miyaura coupling due to the reduced number of functional group interconversions.

One year later, in 2006, Cameron et al. reported an alternative synthesis for a GABA $\alpha_{2,3}$-agonist drug candidate **62** to support clinical trials (Scheme 15B).[60] Similarly to the initial synthesis of **59**, the Suzuki–Miyaura coupling had to be replaced, since the required boronic acid was expensive and generated waste. Therefore, although incorrectly labelled as "Heck-type" mechanism (vide supra), the authors developed a multigram scale C–H activation method, by coupling a similar heterocycle **60** with aryl chloride **61**. The authors propose that by using Bu_4NHSO_4 as additive, anionic Pd^0 species are stabilized, leading to catalyst turnover. Reaction optimization showed that 2-arylated product resulting from a Dimroth rearrangement and bis-aryl by-products could be avoided by using 1,4-dioxane as solvent at 90 °C. The boronic acid coupling partner was exchanged for aryl chloride **61**, lowering the cost and increasing the atom economy of the method. The C–H arylated product **62** was obtained in 87 % yield after recrystallization. Despite similarities between both GABA $\alpha_{2,3}$-agonist **59** and **62**, the 10 g scale synthesis of **58** requires a lower ligand/metal loading than the 5 g C–H arylation towards **62**. This proves that C–H activation steps can be upscaled and high-yielding using low catalyst loadings. Both approaches do not rely on column chromatography and chemical oxidants, leading to reduced waste generation.

Studies in primates from 2013 and 2016, have shown that 3-PCB (**64b**) and 3-ISOPBC (**67**) are potential therapeutic targets to treat alcohol abuse and dependence.[61] In addition, βCCt (**64a**) has shown promising results in rats.[62] To support these studies, scalable synthetic routes were developed to synthetize these carboline derivatives (Scheme 16).

In 2011, Cook et al. documented the synthesis of 3-PCB and βCCt via an intramolecular Pd-catalyzed C–H arylation (Scheme 16A),[63] despite being regarded as a Heck-type mechanism (see discussion above). During optimization of the C–H activation step, the authors observed that switching the base from NaO*t*Bu to K_2CO_3 still afforded a mixture of regioisomers (**64** and **65**) but in a separable ratio. Ultimately, under inert conditions, a 10 g scale C–H arylation of **63** afforded βCCt (**64a**) in 56 % yield, and in a 20 g scale C–H activation step, 3-PCB (**64b**) was obtained in 58 % yield. Taking into account the limitations of the method, especially the lack of regioselectivity, the same authors developed a novel disconnection approach in 2015 (Scheme 16B).[64] By switching the chlorine atom to the pyridine ring **66**, high yields and high selectivity were obtained, without the presence of side-products. Ultimately, 3-ISOPBC (**67**) was synthetized via an intramolecular C–H arylation in a 20 g scale, in 92 % yield after column chromatography. The authors comment that this method could be even scaled up to 50–100 g, however without any further data. βCCt (**64a**) and 3-PCB (**64b**) were also synthetized via this methodology in a smaller scale, leading to 50 % yield (2 g scale) and 92 %

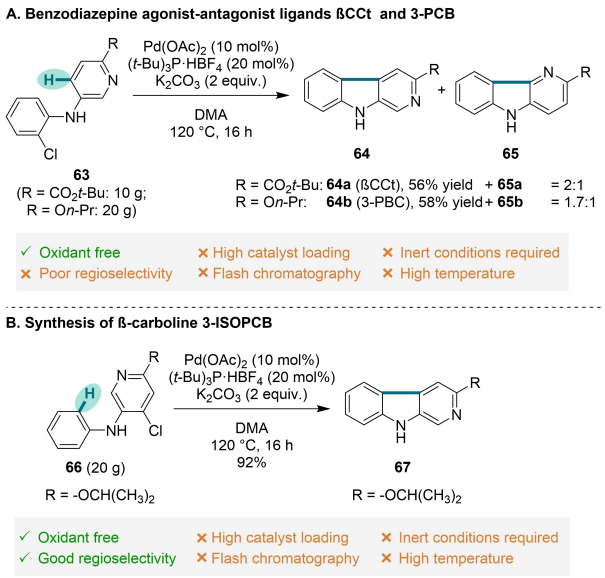

Scheme 16. Intramolecular Pd-catalyzed arylation in A) the synthesis of βCCt (**64a**) and 3-PCB (**64b**), as well as B) the synthesis of ß-carboline 3-ISOPCB (**67**).

© 2023 The Authors. Angewandte Chemie International Edition published by Wiley-VCH GmbH

15213773, 2023, 45, Downloaded from https://onlinelibrary.wiley.com/doi/10.1002/anie.202306659 by Christian-Albrechts-Universitat, Wiley Online Library on [22/01/2025]. See the Terms and Conditions (https://onlinelibrary.wiley.com/terms-and-conditions) on Wiley Online Library for rules of use; OA articles are governed by the applicable Creative Commons License

yield (526 mg scale) respectively after column chromatography. The avoidance of side product formation makes the latter conditions (Scheme 16B) more attractive. However, it should be noted that the high metal and ligand loading (10/20 mol%) in both approaches, may become cost prohibitive when scaling up the process even further.

In 2018, a faster synthetic route to obtain BMS-919373 (**70**) was developed by Savage et al. using a late stage Pd-catalyzed directed C–H arylation (Scheme 17A).[65] At that stage, the API **70** was considered as a potent IKur inhibitor for the treatment of atrial fibrillation. In the initial synthesis, the quinazoline core of **70** was functionalized through the use of well-established reactions, such as aromatic substitutions or cross couplings. In an attempt to avoid lengthy prefunctionalization of substrates, the authors hypothesized that using picolyl amine as a native DG, a direct arylation at C-5 of the quinazoline ring in **68** could be achieved via C–H activation.

During reaction optimization, and in agreement with subsequent mechanistic studies from Wisniewski et al.,[66] some ligands (phosphines, pyridines, phosphites) and solvents (DMF, DMA) completely suppressed the reaction due to a strong coordination with the metal catalyst. Regarding coupling partners, iodobenzene was superior to bromobenzene and phenyltriflate, (the lower bond strength led to a lower activation energy). To prevent product dimerization, solvent and headspace were degassed. The key C–H activation step was performed on a 40 g scale, giving **69** in 78% yield with less than 20 ppm of Pd, when adding ethylene diamine as scavenger during recrystallization. In a subsequent report, Wisniewski et al. reported that the same reaction can be performed in 6.5 kg scale (three batches) with average yields of 76%.[66] While investigating the C–H arylation mechanism in-dept, the authors documented that increasing amounts of base led to the formation of an impurity, resulting from a second C–H activation event: the product could undergo an intramolecular C–H amination step forming a tetracycle **71**, due to the close proximity between the metal and the aryl C–H bond (Scheme 17B). The serendipitously discovered dual C–H activation protocol was optimized, and a 2 g reaction scale was performed, giving **71** in 75% yield, without the use of inert conditions or column chromatography. Contrary to many examples described in the present review, this protocol uses iodobenzene as oxidant to reoxidize Pd^0 to Pd^{II}, leading to more waste. On the other hand, this study exemplifies how detailed mechanistic studies and characterization of reaction impurities can serve as a highly useful tool in upscaling.

In 2018, Zhang et al. developed a convergent synthetic route for the synthesis of GDC-0908 (**74**), a therapeutic development agent for cancer treatment (Scheme 18).[67] The most recent studies, from 2021, show that the API is in Phase I/II for the treatment of solid cancers.[68] The discovery route of **74** had an overall yield of 1%. Despite allowing late-stage diversification of a key intermediate for subsequent SAR studies, a more efficient synthesis was required. Therefore, the authors decided to implement two palladium-catalyzed reactions as key steps: an intramolecular C–H activation and a Negishi coupling. As a starting point to optimize the C–H activation step with **72** as substrate on a 200 mg scale, $Pd(OAc)_2$ (5 mol%) was used as catalyst with 1,1′-bis(diphenylphosphino)ferrocene (dppf) (10 mol%) as ligand, in DMF at 100 °C. In contrast to organic bases, inorganic bases such as Cs_2CO_3 and K_2CO_3 gave quantitative conversion, with CsOAc (1 equiv.) being the optimal choice. When metal and ligand loading were decreased (1 mol% and 2 mol% respectively), in combina-

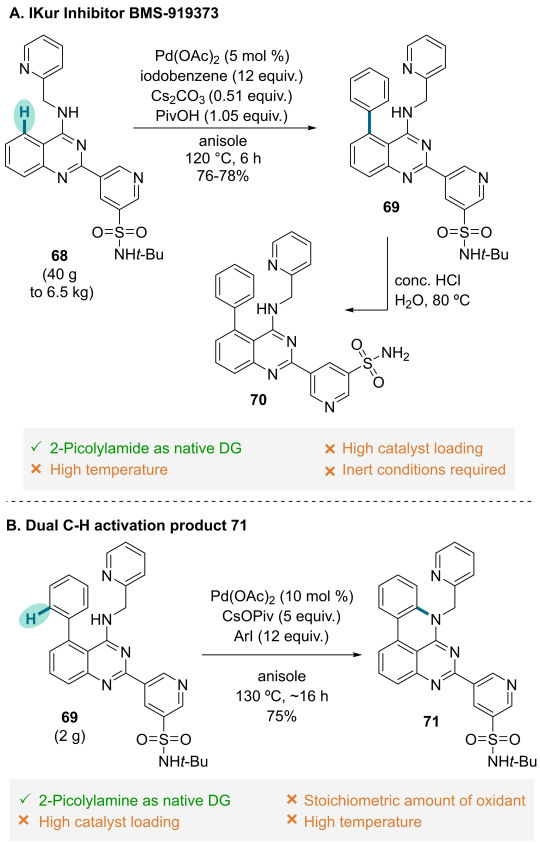

Scheme 17. A) Directed Pd-catalyzed arylation in the synthesis of BMS-919373 (**70**). B) Tetracycle formation **71** via intramolecular C–H activation step.

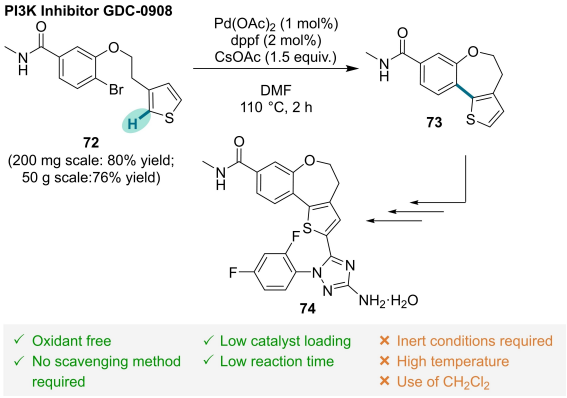

Scheme 18. Synthesis of GDC-0908 (**74**) via intramolecular Pd-catalyzed direct arylation.

© 2023 The Authors. Angewandte Chemie International Edition published by Wiley-VCH GmbH

15213773, 2023, 45, Downloaded from https://onlinelibrary.wiley.com/doi/10.1002/anie.202306659 by Christian-Albrechts-Universitat, Wiley Online Library on [22/01/2025]. See the Terms and Conditions (https://onlinelibrary.wiley.com/terms-and-conditions) on Wiley Online Library for rules of use; OA articles are governed by the applicable Creative Commons License

tion to higher reaction temperature (110 °C) and higher base loading (1.5 equiv.), the tricyclic dihydrobenzothienooxepine heterocycle **73** was obtained in 82 % assay yield, and in 80 % yield after column chromatography. Using $PdCl_2$(dppf) as an alternative Pd^{II} source, lead to equal assay yields. The intramolecular C–H activation step was performed on a 50 g scale with 76 % yield, after extractions and filtration over a pad of silica gel (using dichloromethane and dichloromethane/ethylacetate mixtures), occurring in the electronically preferred 2-position. Taking into account that two transition metal-catalyzed reactions were executed and several heteroatoms are present in the molecule, it is remarkable that the final API **74** had less than 20 ppm metal traces without the use of any scavenging method. Despite the use of high temperatures, the good yields obtained with 1 mol% of metal catalyst in only 2 h reaction time, renders this method cost and time efficient.

LY2784522 (**78**) is an API in Phase II studies for the treatment of several myeloproliferative disorders.[69] Several drawbacks in the original synthesis,[70] such as the lack of readily accessible reagents, the presence of impurities and waste disposal issues, encouraged Campbell et al. to develop a novel synthetic route (Scheme 19).[71] To achieve the C-3 benzylation of the imidazopyridazine moiety **75**, the authors proposed two efficient and atom economical approaches: either via decarboxylative benzylation or via direct C–H benzylation. In 2009, Fagnou et al. described a palladium-catalyzed benzylation of heteroarenes, showing that Csp^2-Csp^3 bond formation can be attained although less investigated than Csp^2-Csp^2 bond formation.[72] Since decarboxylative benzylation experiments lead to the formation of several by-products and only traces of **77**, C–H activation was explored. Ligand and base screening showed that PPh_3 and K_2CO_3 were optimal. Screening of Pd^{II} sources proved that the anionic and basic ligands were essential for reactivity: $Pd(OAc)_2$ was superior to $Pd(TFA)_2$, most likely because of the higher basicity of the acetate ligand. The authors propose a CMD mechanism. $Pd(OPiv)_2$ afforded slightly lower yields in comparison to $Pd(OAc)_2$. $PdCl_2$ provided substantially lower yields, but similar yields to $Pd(OAc)_2$ were obtained in combination with 10 % NaOAc. When K_2CO_3 was replaced with NaOAc, almost no product formation was observed, suggesting catalyst poisoning, with excess acetate. The same outcome occurred when PivOH was tested as additive, indicating the sensitivity of the reaction to the stoichiometry of carboxylate ligands. Solvent replacement to a less toxic one was attempted, but while anisole provided good yields, 1,4-dioxane remained the best option. Using as optimized conditions, $Pd(OAc)_2$ (5 mol%), PPh_3 (10 mol%), and K_2CO_3 in dioxane at 101 °C for 16 h, a yield of 70 % was obtained (85 % conversion). Increasing reaction time or catalyst loading did not improve the yields. Catalyst poisoning can be excluded since spiking the reaction with the product or impurity did not influence the yield. Using **76** as coupling partner, C–H activation on a 273 g scale afforded **77** in 50 % yield. The use of a toxic solvent in addition to high catalyst loading are key drawbacks of this method. However, the authors show that implementing a "high risk, high reward" strategy, enabled the selective C-3 benzylation (most electron-rich position) which was impossible to obtain using the decarboxylative benzylation approach.

In the present review, several examples of direct C–H arylation of heterocycles have been described, highlighting not only the importance of such motifs in medicinal chemistry,[73] but also the utility of C–H activation in this context. In 2016, Kuroda et al. developed a protocol for the synthesis of PDE4 inhibitor **82**, a molecule expected to counteract memory loss (Scheme 20).[74]

The main issues present in the first-generation route were the length of the synthetic route and the use of hazardous chemicals (mutagenic 2-aminophenol). To overcome these hurdles, non-directed C–H arylation was implemented in the second-generation route. Inspired by the work of Miura et al.,[75] copper salt additives were screened in combination with $Pd(OAc)_2$ (10 mol%) and PPh_3 (24 mol%) in NMP. The authors observed that the Lewis acidity of the copper salt correlated with reactivity, most likely due to benzoxazole activation: Cu^{II} salts like CuO, $CuBr_2$ and $Cu(OTf)_2$ led to increased yields in

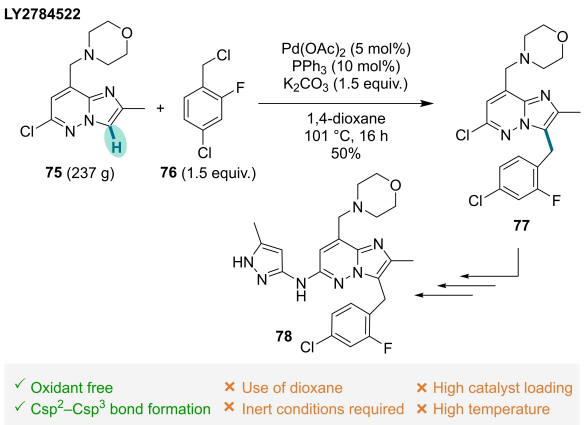

Scheme 19. Synthesis of LY2784522 (**78**) via Pd-catalyzed direct benzylation.

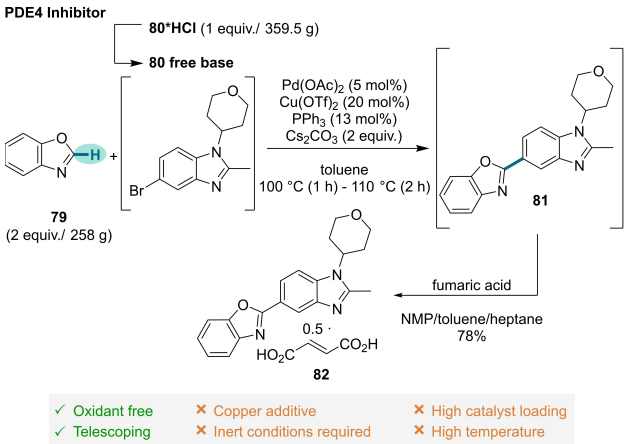

Scheme 20. Synthesis of PDE4 inhibitor **82** via Pd-catalyzed direct arylation.

© 2023 The Authors. Angewandte Chemie International Edition published by Wiley-VCH GmbH

15213773, 2023, 45, Downloaded from https://onlinelibrary.wiley.com/doi/10.1002/anie.202306659 by Christian-Albrechts-Universitat, Wiley Online Library on [22/01/2025]. See the Terms and Conditions (https://onlinelibrary.wiley.com/terms-and-conditions) on Wiley Online Library for rules of use; OA articles are governed by the applicable Creative Commons License

comparison to $Cu(OAc)_2$ and no arylated product was formed when $Cu(OTf)_2$ was used in the absence of $Pd(OAc)_2$. Based on price, availability, and reactivity, $Cu(OTf)_2$ was chosen as additive. To improve green chemistry metrics, NMP was exchanged to toluene (to promote crystallization), and metal loading was reduced by half, without further information on the optimization of the Pd-source. Ligand screening showed that PPh_3 and $PtBu_3$ displayed similar reactivity, of which PPh_3 was selected, most likely due to its lower cost and higher stability. Optimization of the ligand-to-metal ratio indicated that a ratio of 2.5 prevented the formation of undesired side products, without undermining reactivity. As a proof of concept, a 10 g scale C–H activation reaction led to the desired compound **81** in 94% yield. Ultimately, the optimized C–H activation protocol was implemented on a 258 g scale and telescoped. Using **79** and previously telescoped **80**, **82** was obtained in 78% (HPLC assay yield), after treating with fumaric acid and subsequent crystallization. Owing to the use of telescoping methods, column chromatography steps were reduced, generating less waste. In addition, the absence of mutagenic reagents, renders the second-generation route superior to the original synthesis.

With the aim to establish novel methods for heteroarenes C–H arylation, Huang et al. developed a Pd/Cu catalytic system ($[(t\text{-Bu})_2PCl]_2PdCl_2$ (0.25 mol%) and Cu(Xantphos)I (1 mol%)) in 2010.[76] As a mechanistic proposal, the authors suggest that transmetallation between the copper species and a Pd^{II} species is the key step. This protocol was recently applied by Walker and co-workers to support the $S1P_1$ program, with AMG 369 (**86**) as a promising $S1P_1$ agonist (Scheme 21).[77]

To replace its multistep original synthetic route,[78] non-directed C–H arylation of benzothiazole **83** using the dual catalytic system by Huang et al. was performed on a multikilogram scale (2.1 kg). Using as coupling partner **84**, the arylated product **85** was obtained in 71% yield.[76] Despite employing two metal sources, the low catalyst loading, and absence of an external oxidant are notable strengths of this protocol. Even though the authors describe a novel retrosynthetic approach to afford the arylated benzothiazole core of AMG 396, a complete synthetic route to obtain **86** or other $S1P_1$ agonist is not reported. Considering the API structure and their C–H arylation scope, no halide coupling partner with a fluorine atom on the arene 2-position was tested, indicating that further functionalization of the aromatic ring is required. Even though the authors increased the applicability of the method reported by Huang et al., the lack of information about the following steps to obtain **86**, does not help the readers understand the outcome of this investigation.

YLF466D (**90**) is a drug candidate for the treatment of metabolic diseases and myocardial ischemia-reperfusion injury.[79] In the discovery route, the authors applied a palladium domino intermolecular carbopalladation/C–H activation/C–C bond formation protocol based on previous work from Zhu et al.[80] However, the reaction suffered from low selectivity, giving undesired isomer and dehalogenated product. Further drawbacks, such as low yields and use of column chromatography further undermined the applicability of the discovery route. Therefore, to supply API **90** in a multikilogram scale for clinical trials, Nan, Zhang and co-workers decided to improve the synthetic route, using a C–H activation step as key part of the new sequence (Scheme 22). Screening of Pd sources, bases, solvent, and temperature were performed to avoid side product formation: $Pd(dppf)Cl_2 \cdot CH_2Cl_2$ was the optimal metal catalyst in comparison to $Pd(OAc)_2$, $Pd(PPh_3)_4$, $Pd(dba)_2$. Exchanging the initial solvent DMF to MeCN and K_2CO_3 in combination with the $Pd(dppf)Cl_2 \cdot CH_2Cl_2$, afforded higher product selectivity in comparison to CsF. Lowering the reaction temperature (60 °C instead of 82 °C) did not significantly reduce impurity formation. Under the optimized conditions ($Pd(dppf)Cl_2 \cdot CH_2Cl_2$ (3 mol%), K_2CO_3, MeCN at 82 °C), a 5 g scale C–H activation with **87** and **88** yielded **89** in 74% after column chromatography. For a more sustainable purification, the authors developed a recrystallization process, and ethylenediaminetetraacetic acid (EDTA) tetrasodium salt was used as chelator to remove transition metal traces. When performing the C–H activation step on a 5 kg

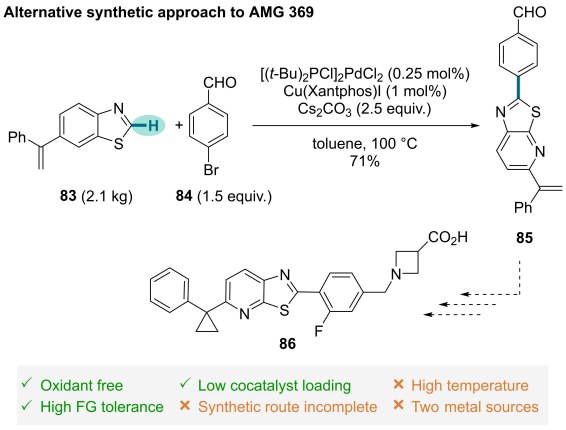

Scheme 21. Synthesis of intermediate **85** via Pd-catalyzed direct arylation as a possible synthetic approach for the synthesis of AMG 369 (**86**).

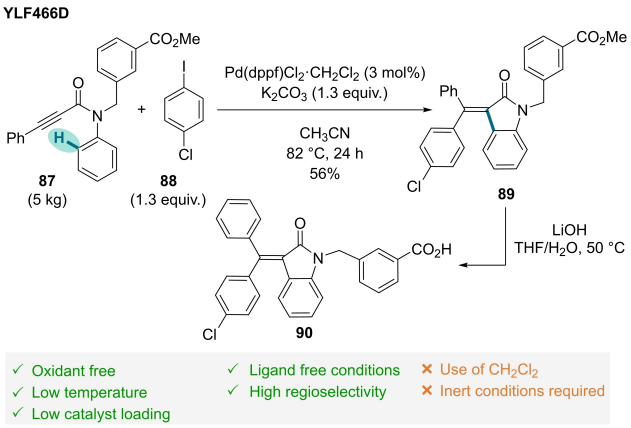

Scheme 22. Synthesis of YLF466D (**90**) via Pd-catalyzed direct arylation.

© 2023 The Authors. Angewandte Chemie International Edition published by Wiley-VCH GmbH

15213773, 2023, 45, Downloaded from https://onlinelibrary.wiley.com/doi/10.1002/anie.202306659 by Christian-Albrechts-Universitat, Wiley Online Library on [22/01/2025]. See the Terms and Conditions (https://onlinelibrary.wiley.com/terms-and-conditions) on Wiley Online Library for rules of use; OA articles are governed by the applicable Creative Commons License

scale, followed by recrystallization, high purity **89** was obtained in 56 % yield, with side products bellow 0.1 area% by HPLC. In agreement with Zhu et al., the regioselectivity of the process results from the carbopalladation step. The regioselective addition of the aryl group to the α-position of the ynamide moiety can be explained by the intramolecular nature of this step, in which this regioselectivity is favored according to the Baldwin rules.[81] Despite the use of dichloromethane during workup, the low ligand loading and the absence of additional ligand and oxidant, make this approach cheaper and more sustainable than alternative routes.

In 2003, Buchwald et al. developed a palladium-catalyzed C–H activation protocol for the synthesis of substituted oxindoles, using α-chloroacetanilide precursors as starting materials.[82] This method ($Pd(OAc)_2$ as metal catalyst, 2-(di-*tert*-butylphosphino)biphenyl as ligand, triethylamine as base, in toluene at 80 °C) represents a mild alternative to Friedel-Craft- type protocols, which are characterized by high temperatures and acidic conditions. Inspired by this transformation, and using oxindoles as advanced intermediates, two APIs (**93** and **97**) were synthetized on a large scale (Scheme 23).

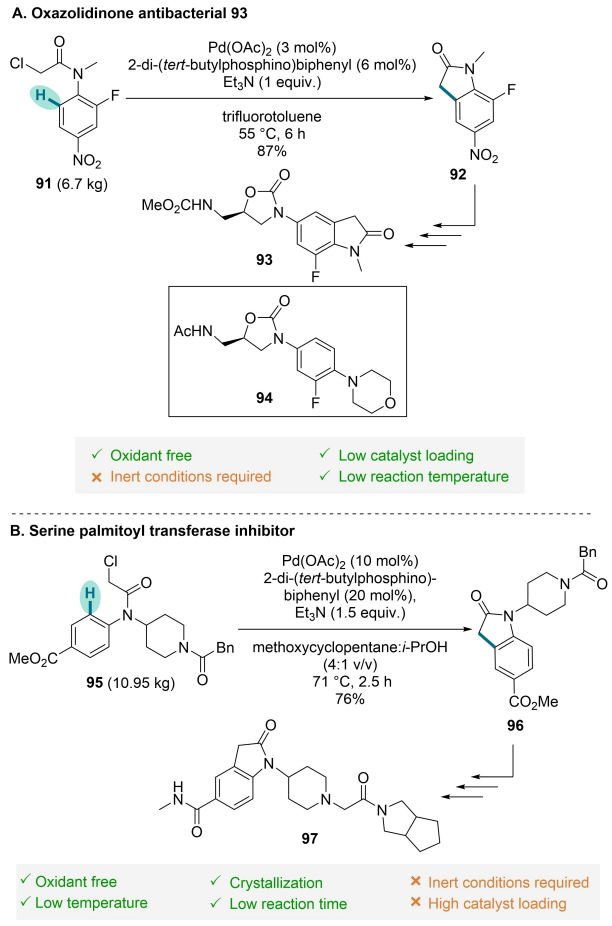

Scheme 23. A) Oxindole formation via Pd-catalyzed direct arylation in the A) synthesis of oxazolidinone antibacterial **93** and B) serine palmitoyl transferase inhibitor **97**.

Linezolid (**94**) belongs to the class of oxazolidinone antibiotics (Scheme 23A).[83] However, its undesirable side effects[84] prompted Pamment et al. to develop a safer alternative that could easily progress into Phase II clinical trials.[85] Therefore, an efficient synthetic route to obtain **93** was pursued (Scheme 23A). To cyclize **91** and obtain the oxindole core **92**, the conditions reported by Buchwald were initially investigated. Due to significant decomposition, reaction parameters were optimized. To address concerns regarding the base and temperature sensitivity of **92**, trifluorotoluene was employed as solvent.

After 5 h, complete conversion was obtained, giving the product **92** in approximately 75 % yield. This choice of solvent proved to be beneficial in comparison to DMF, due to its lower boiling point and lower cost. In agreement with Buchwald's initial report, 2-(di-*tert*-butylphosphino)biphenyl was the optimal ligand, while other ligands such as 2-(dicyclohexylphosphino)biphenyl or $P(t\text{-}Bu)_3HBF_4$ only afforded traces of product. To enable a more cost-effective transformation, metal and ligand loading (3 and 6 mol% respectively) were reduced, but conversion dropped to less than 40 %. Considering the readily accessible ligand and the amount of API required for that drug development stage, the authors did not proceed with further optimization. This illustrates the fact that depending on the stage of drug development, the goals and priorities vary. Therefore, intramolecular C–H activation was performed on a 6.7 kg scale, leading to the desired product **92** in 87 % yield. The authors acknowledge that further optimization to reduce the metal loading is necessary for future applications. Additionally, a broader screening of ligand, additives, solvents, and metal sources could likely lead to a more efficient catalytic system.

Similar reaction conditions but on a larger scale were applied in the synthesis of **97** (Scheme 23B), a potential API for the treatment of heart disease.[86] The medicinal chemistry route towards **97** had some disadvantages, such as the use of strong bases, purifications via column chromatography and a high cost starting material.[87] To circumvent those problems, whilst providing enough material for clinical trials, Magano et al. envisioned a more step-economical synthetic route.[88] Using **95** as starting material, optimization of the palladium-catalyzed C–H activation step was initiated. When applying the conditions by Buchwald and coworkers,[82] formation of sticky solids prevented good stirring, leading to poor reaction homogeneity. By switching toluene to a mixture of 4:1 (2-MeTHF/2-propanol) at 70–80 °C, solids were still present, but the reaction mixture was more homogeneous and easier to stir. As a result, **96** was obtained in 70 % yield on a gram scale, in less than 1 h. Attempts to reduce the metal/ligand loading (10 and 20 mol% respectively) by half, resulted in impurity formation, and conversions stalling at 80–85 %. Therefore, using $Pd(OAc)_2$ with 2-di-(*tert*-butylphosphino)biphenyl as ligand, and triethylamine as base, the intramolecular C–H activation was performed multiple times on a 25–50 g scale, twice on a 5 kg scale, and once on a 10 kg scale, with yields ranging from 76 to 84 %. To avoid column chromatography, filtration followed by recrystallization was the purification method of choice, with metal traces between 100–800 ppm.

© 2023 The Authors. Angewandte Chemie International Edition published by Wiley-VCH GmbH

15213773, 2023, 45, Downloaded from https://onlinelibrary.wiley.com/doi/10.1002/anie.202306659 by Christian-Albrechts-Universitat, Wiley Online Library on [22/01/2025]. See the Terms and Conditions (https://onlinelibrary.wiley.com/terms-and-conditions) on Wiley Online Library for rules of use; OA articles are governed by the applicable Creative Commons License

The development of this protocol expanded the substrate scope of Buchwald's initial report (**95** contains a Cbz-PG) and demonstrated that a different ligand can be employed efficiently. On a 25 g scale, the authors tested 5-(di-*tert*-butylphosphino)-1′,3′,5′-triphenyl-1′*H*-[1,4′]-bipyrazole (Bippyphos) under the same reaction conditions described in Scheme 23B and the desired product **96** was isolated in 84 % yield. Even though a high catalyst loading is still required, this method alleviated the key disadvantages from the medicinal chemistry route.

As previously discussed in Scheme 10, the potential long term manufacturing route of nemiralisib (**38**) is based on two consecutive C–H activation steps to form two biaryl bonds.[44] To functionalize the 2-position of the oxazole scaffold, Pd-catalyzed C–H activation was investigated (Scheme 24).

In preliminary studies, with oxazole ester and 4-bromoindazole as coupling partners, a combination of $Pd(OAc)_2$, RuPhos, pivalic acid and Cs_2CO_3 in toluene, did not afford the desired product. This can be explained by catalyst poisoning due to the binding of the indazole N–H bond to the metal catalyst. Under the same reaction conditions, a screening of PGs showed that applying base-stable PGs, such as tetrahydropyran (THP) or *p*-methoxybenzyl, lead to the formation of biaryl product. As mentioned in the discussion of Scheme 10, during route scouting, the substrate for borylation was modified. Changes were driven by the development of a more convergent route to access **98** as starting material for the Pd-catalyzed C–H activation. In addition to that, indazole chloride **99** was selected as coupling partner to decrease costs. During further optimization studies, RuPhos was exchanged with the cheaper XPhos. Testing of other ligands such as Cy_2PPh lead to undesired side products. By replacing $Pd(OAc)_2$ with $PdCl_2$, the metal loading could be reduced from 5 mol% to 2.8 mol%, and the ligand loading from 10 mol% to 6 mol%. Cyclopentyl methyl ether proved to be the optimal solvent since reaction, workup, and isolation could be performed in the same solvent. Using **98** on a 34.8 kg scale, the Pd-catalyzed arylation was performed, giving **36** in 89 % yield. The changes performed while stablishing the route show that challenges such as the cost of reagents and the sustainability of a process (convergence of the route), can be addressed by implementing C–H activation steps. The low catalyst loading in both reactions, in combination with the scale in which the reactions were performed, are prime examples of upscaling C–H activation in API synthesis.

In 2020, LSZ102 (**103**) was a drug candidate in Phase I/IB for the treatment of estrogen receptor α-positive breast cancer.[89] To meet increased API demand, Baenziger et al. developed an efficient chemical synthesis (Scheme 25).[90]

During route scouting, a potential strategy was based on a late-stage Negishi cross-coupling. However, protection of the free carboxylic acid and the generation of zinc waste were limitations of this approach. As an alternative, the authors envisioned a palladium-catalyzed C–H activation step between **100** and **101**. Without further information about reaction optimization, using $Pd(OAc)_2$ (4 mol%), PPh_2Cy (8 mol%), NaO*t*Bu as base, and dicyclohexylamine

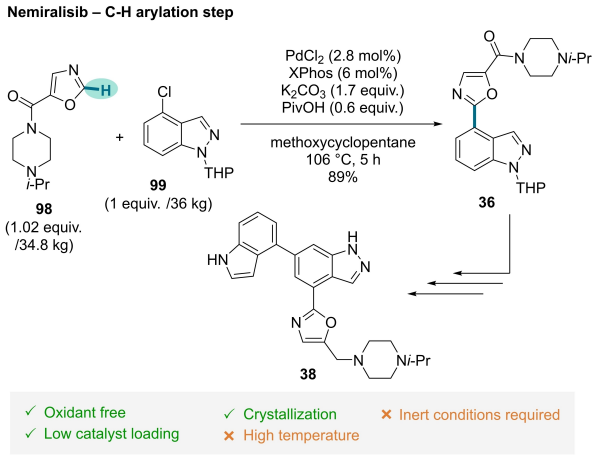

Scheme 24. Pd-catalyzed C–H arylation step in the synthesis of nemiralisib (**38**).

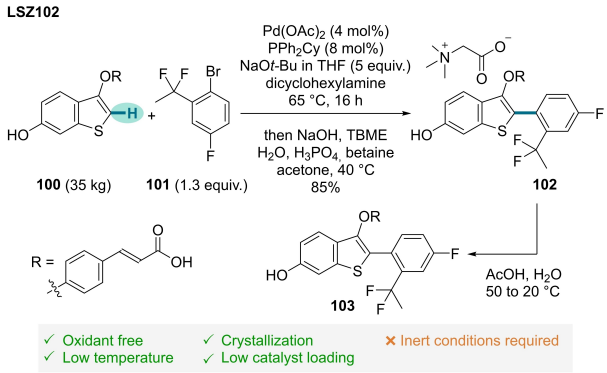

Scheme 25. Synthesis of LSZ102 (**103**) via Pd-catalyzed direct arylation.

as solvent, the desired product **102** was formed with high conversion (less than 2 % of starting material **100** left). When recrystallized **100** was used, the metal (2 mol% $[Pd(C_3H_5)Cl]_2$) and ligand (4 mol%) loading could be reduced. However, no yields were reported, and the authors did not proceed with these conditions. The reaction outcome was influenced by several factors such as the water content (below 400 ppm required), use of inert conditions, and the quality of $Pd(OAc)_2$. The immediate product from C–H activation was not isolated. Instead, a stepwise purification process which included conversion of the crude C–H activation product to the betaine co-crystal **102**, enabled the purging of impurities. On a 35 kg scale, Pd-catalyzed C–H activation led to **102** in 85 % yield, with metal levels below 3 ppm. Subsequently, the crystalline API **103** can be obtained from an acetic acid/H_2O system in 76 % yield. The authors also identified 3-mercaptopropyl ethyl sulfide silica as a suitable Pd scavenger that could be used in future manufacturing processes. Using C–H activation as an alternative disconnection approach, the substrate prefunctionalization required for a Negishi coupling was avoided, decreasing step count and giving a more efficient overall route.

© 2023 The Authors. Angewandte Chemie International Edition published by Wiley-VCH GmbH

15213773, 2023, 45, Downloaded from https://onlinelibrary.wiley.com/doi/10.1002/anie.202306659 by Christian-Albrechts-Universitat, Wiley Online Library on [22/01/2025]. See the Terms and Conditions (https://onlinelibrary.wiley.com/terms-and-conditions) on Wiley Online Library for rules of use; OA articles are governed by the applicable Creative Commons License

Another kilogram scale C–H activation step was implemented in the convergent synthesis of beclabuvir (**106**), a potential drug candidate for the treatment of hepatitis C virus.[91] Inspired by work from Kosikowski and co-workers,[92] the authors envisioned a palladium-catalyzed intramolecular cyclization to form the seven-membered ring (Scheme 26).

This novel retrosynthetic approach would obviate functional group manipulations, streamlining the synthetic route. In this study, the reaction conditions for the C–H activation reaction were optimized using a simplified model substrate. The such developed reaction conditions (5 mol% $Pd(OAc)_2$, 10 mol% $PCy_3 \cdot HBF_4$, and KOAc in dimethylacetamide (DMAc)), proved to be robust once applied to the final substrate **104**, producing 9.14 kg of the target compound (68 % yield). However, a tedious workup procedure, high vacuum distillation of DMAc, and considerable residual Pd levels (around 110 ppm over 3 batches), prompted the authors to further optimize the conditions. The base was exchanged to $KHCO_3$, resulting in a decrease in reaction time (from 12–16 h to less than 4 h), and a mixture of DMAc:toluene (1:1) was used as solvent. Under the newly optimized conditions, the C–H activation step was carried out on a 42.8 kg scale, and ester hydrolysis under basic conditions was performed after the reaction was completed. Filtration of palladium black, followed by a simpler workup (not involving DMAc distillation) and recrystallization, gave product **105** in 85 % yield. This protocol was used to obtain a total 139 kg of **105**, with metal traces below 100 ppm. Despite the high catalyst loading, the intramolecular formation of a polycyclic indole **105** and a broad functional group tolerance are strengths of this method.

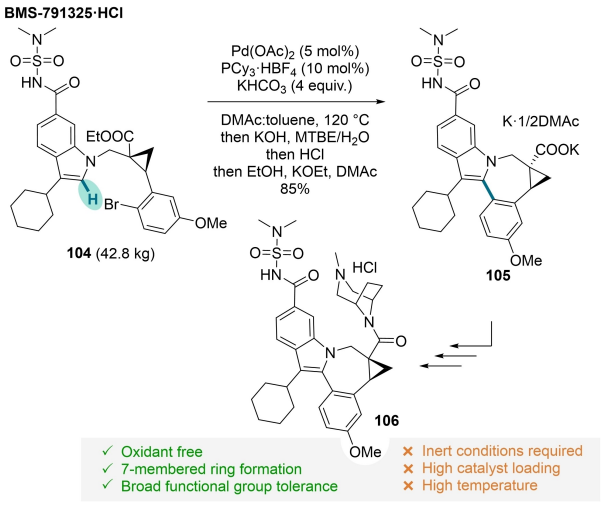

Scheme 26. Intramolecular Pd-catalyzed direct arylation in the synthesis of beclabuvir (**106**).

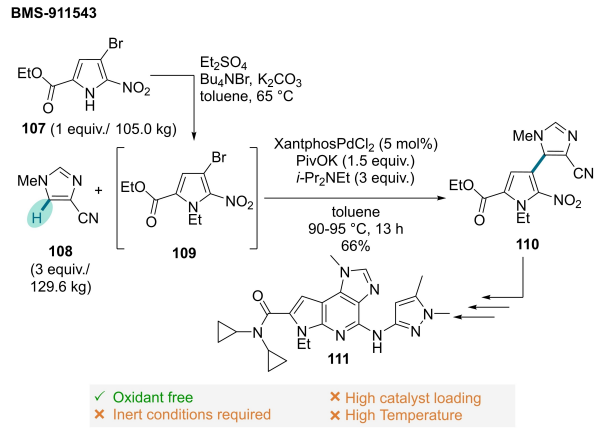

Scheme 27. Synthesis of BMS-911543 (**111**) via Pd-catalyzed direct arylation.

In 2015, BMS-911543 (**111**) was undergoing clinical trials as a potential treatment for myeloproliferative disorder (Scheme 27).[93] One of the limitations of the first-generation route towards this compound was substrate prefunctionalization required for the Suzuki–Miyaura cross-coupling.[94] In 2018, Fox, Cuniere and co-workers envisioned a long term commercially efficient synthetic route to overcome this drawback by using a palladium-catalyzed C–H heteroarylation step.[95] To avoid catalyst poisoning, the pyrrole N–H group **107** was protected by ethylation. Initially, using 4–5 mol% $Pd(PPh_3)_2Cl_2$, K_2CO_3 and DMAc at 90 °C and **108** as starting material, only 28 % conversion were obtained. An additive screening showed that bulkier carboxylates reduced the reaction rate, suggesting a CMD-type mechanism. Further investigation revealed that a dual base system of *i*-Pr_2NEt and PivOK gave a homogeneous reaction mixture and reduced the formation of impurities, stemming from side reactions of the ester from coupling partner **109**.

To improve conversion and selectivity, metal and ligand combinations were investigated. While $Pd(PPh_3)_2Cl_2$: PPh_3 (1:2) and $Pd(OAc)_2$: PPh_3 (1:5) were unsuccessful, the use of a bidentate ligand in $Pd(Xantphos)Cl_2$ improved the reaction rate and gave low side-product formation. Based on mechanistic studies,[96] the formation of a hemilabile system is proposed, which would deliver high activities and at the same time suppress decomposition during catalyst turnover. Once the C–H activation reaction conditions were optimized ($Pd(Xantphos)Cl_2$ (5 mol%), *i*-Pr_2NEt/PivOK, and Bu_4NBr in toluene), the ethylation and C–H heteroarylation steps were telescoped. The C–H activation was performed on a 129.6 kg scale, giving **110** in 66 % yield and with high regioselectivity (>50:1 C5:C2). Through a series of heat cycles, **110** could be obtained in high purity. Interestingly, the use of telescoping methods in this synthesis reduces the overall number of isolation steps, making the method more straightforward and eco-friendlier. This protocol shows that the application of C–H activation technology, avoiding the use of prefunctionalized starting materials, can be implemented on industrial scales.

3. Summary and Outlook

The development of efficient synthetic routes with high atom economy that can rapidly deliver APIs, is a key challenge in the pharmaceutical industry. In this review, we have highlighted how C–H activation can serve as a key

© 2023 The Authors. Angewandte Chemie International Edition published by Wiley-VCH GmbH

15213773, 2023, 45, Downloaded from https://onlinelibrary.wiley.com/doi/10.1002/anie.202306659 by Christian-Albrechts-Universitat, Wiley Online Library on [22/01/2025]. See the Terms and Conditions (https://onlinelibrary.wiley.com/terms-and-conditions) on Wiley Online Library for rules of use; OA articles are governed by the applicable Creative Commons License

technology to achieve this goal, reducing the length of synthetic sequences and waste production. The examples discussed herein show that major challenges need to be addressed when applying C–H activation on preparatively relevant scales, but also highlight the strategies that can be used to overcome such hurdles. The proper choice of DG, carefully optimized reaction conditions and catalyst design, are some factors to keep in mind when designing selective C–H activation methodologies. Various APIs can now be synthesized with C–H activations as key steps on scales sometimes exceeding 100 kg, delivering significant improvements compared to routes using traditional cross-coupling approaches. As discussed herein, important considerations when scaling up C–H activations include the reduction of catalyst loadings, the avoidance of external oxidants, the need for high selectivities and the control of product purity (trace metals). The studies presented above demonstrate that all of these requirements can be met in process development, and thus pave the way for future implementations of C–H activation in the production of pharmaceuticals. As with other key technologies, time and research efforts are required to achieve the transition from methods developed in basic research laboratories on milligram scales to preparatively useful applications. A key future challenge will be to implement inherently oxidative C–H activation methodologies on scale. Towards this, the synergistic combination of C–H activation with enabling technologies such as electrochemistry and/or photochemistry, as well as flow-chemistry are important areas of research that bear the potential to pave the way for many further environmentally friendly applications of C–H activation in the pharmaceutical industry.[6d] The examples described in this review are thus expected to be a foretaste to developments in the coming years, where C–H activation will be crucial for a sustainable and economically viable development of pharmaceutical synthesis.

Acknowledgements

The authors acknowledge generous financial support by the DFG (Walter-Benjamin Programme HI 2351/1-1), Kiel University, and the European Research Council (ERC) under the European Union's Horizon 2020 research and innovation programme (grant agreement No 946044). Open Access funding enabled and organized by Projekt DEAL.

Conflict of Interest

The authors declare no conflict of interest.

Data Availability Statement

Data sharing is not applicable to this article as no new data were created or analyzed in this study.

Keywords: C–H Activation · Catalysis · Large Scale Synthesis · Pharmaceuticals · Sustainability

[1] a) D. J. Stewart, A. A. Stewart, P. Wheatley-Price, G. Batist, H. M. Kantarjian, J. Schiller, M. Clemons, J.-P. Bradford, L. Gillespie, R. Kurzrock, *Cancer Med.* **2018**, *7*, 1824; b) R. Jana, H. M. Begam, E. Dinda, *Chem. Commun.* **2021**, *57*, 10842.
[2] D. G. Brown, J. Boström, *J. Med. Chem.* **2016**, *59*, 4443.
[3] a) T. Rogge, N. Kaplaneris, N. Chatani, J. Kim, S. Chang, B. Punji, L. L. Schafer, D. G. Musaev, J. Wencel-Delord, C. A. Roberts, R. Sarpong, Z. E. Wilson, M. A. Brimble, M. J. Johansson, L. Ackermann, *Nat. Rev. Methods Primers* **2021**, *1*, 43; b) K. Lovato, P. S. Fier, K. M. Maloney, *Nat. Chem. Rev.* **2021**, *5*, 546.
[4] a) K. Godula, D. Sames, *Science* **2006**, *312*, 67; b) T. Gensch, M. N. Hopkinson, F. Glorius, J. Wencel-Delord, *Chem. Soc. Rev.* **2016**, *45*, 2900; c) F. Roudesly, J. Oble, G. Poli, *J. Mol. Catal. A* **2017**, *426*, 275.
[5] a) K. M. Altus, J. A. Love, *Commun. Chem.* **2021**, *4*, 173; b) J. A. Labinger, J. E. Bercaw, *Nature* **2002**, *417*, 507; c) A. E. Shilov, G. B. Shul′pin, *Chem. Rev.* **1997**, *97*, 2879.
[6] It should be noted that beyond the methods based on C–H activation covered herein, complementary strategies for C–H functionalization have been developed and employed with great success, such as 1,n-hydrogen atom transfer, carbene- or nitrene insertions, photochemistry, electrosynthesis, and enzyme catalysis. For selected reviews on these alternative strategies for C–H functionalization, see: a) J. C. K. Chu, T. Rovis, *Angew. Chem. Int. Ed.* **2018**, *57*, 62; b) S. Sarkar, K. P. S. Cheung, V. Gevorgyan, *Chem. Sci.* **2020**, *11*, 12974; c) N. Holmberg-Douglas, D. A. Nicewicz, *Chem. Rev.* **2022**, *122*, 1925; d) L. Guillemard, N. Kaplaneris, L. Ackermann, M. J. Johansson, *Nat. Chem. Rev.* **2021**, *5*, 522; e) C. Ma, P. Fang, T.-S. Mei, *ACS Catal.* **2018**, *8*, 7179.
[7] For selected reviews on the use of C–H activation in material science, see: a) K. Wang, J. Zhang, R. Hu, C. Liu, T. A. Bartholome, H. Ge, B. Li, *ACS Catal.* **2022**, *12*, 2796; b) I. A. Stepek, K. Itami, *ACS Mater. Lett.* **2020**, *2*, 951; c) Y. Segawa, T. Maekawa, K. Itami, *Angew. Chem. Int. Ed.* **2015**, *54*, 66; d) J. Wencel-Delord, F. Glorius, *Nat. Chem.* **2013**, *5*, 369.
[8] For an overview on the synthesis of natural products via C–H activation see: a) L. McMurray, F. O'Hara, M. J. Gaunt, *Chem. Soc. Rev.* **2011**, *40*, 1885; b) D. J. Abrams, P. A. Provencher, E. J. Sorensen, *Chem. Soc. Rev.* **2018**, *47*, 8925; c) N. Y. S. Lam, K. Wu, J.-Q. Yu, *Angew. Chem. Int. Ed.* **2021**, *60*, 15767; d) J. Yamaguchi, A. D. Yamaguchi, K. Itami, *Angew. Chem. Int. Ed.* **2012**, *51*, 8960; e) O. Baudoin, *Angew. Chem. Int. Ed.* **2020**, *59*, 17798.
[9] For selected reviews on the use of C–H activation for late-stage functionalization in medicinal chemistry, see: a) T. Cernak, K. D. Dykstra, S. Tyagarajan, P. Vachal, S. W. Krska, *Chem. Soc. Rev.* **2016**, *45*, 546; b) J. Boström, D. G. Brown, R. J. Young, G. M. Keserü, *Nat. Rev. Drug Discovery* **2018**, *17*, 709.
[10] A. P. Taylor, R. P. Robinson, Y. M. Fobian, D. C. Blakemore, L. H. Jones, O. Fadeyi, *Org. Biomol. Chem.* **2016**, *14*, 6611.
[11] N. A. M. Tamimi, P. Ellis, *Nephron Clin. Pract.* **2009**, *113*, c125.
[12] a) J. Magano, J. R. Dunetz, *Chem. Rev.* **2011**, *111*, 2177; b) T. Gensch, M. J. James, T. Dalton, F. Glorius, *Angew. Chem. Int. Ed.* **2018**, *57*, 2296; c) T. Dalton, T. Faber, F. Glorius, *ACS Cent. Sci.* **2021**, *7*, 245.
[13] N. Raval, V. Tambe, R. Maheshwari, P. K. Deb, R. K. Tekade, *Dosage Form Design Considerations*, Academic Press, New York, **2018**, p. 669.
[14] E. J. E. Caro-Diaz, M. Urbano, D. J. Buzard, R. M. Jones, *Bioorg. Med. Chem. Lett.* **2016**, *26*, 5378.

© 2023 The Authors. Angewandte Chemie International Edition published by Wiley-VCH GmbH

15213773, 2023, 45, Downloaded from https://onlinelibrary.wiley.com/doi/10.1002/anie.202306659 by Christian-Albrechts-Universitat, Wiley Online Library on [22/01/2025]. See the Terms and Conditions (https://onlinelibrary.wiley.com/terms-and-conditions) on Wiley Online Library for rules of use; OA articles are governed by the applicable Creative Commons License

[15] a) R. Ali, R. Siddiqui, *Adv. Synth. Catal.* **2021**, *363*, 1290; b) C. Sambiagio, D. Schönbauer, R. Blieck, T. Dao-Huy, G. Pototschnig, P. Schaaf, T. Wiesinger, M. F. Zia, J. Wencel-Delord, T. Besset, B. U. W. Maes, M. Schnürch, *Chem. Soc. Rev.* **2018**, *47*, 6603; c) P. Gandeepan, L. Ackermann, *Chem* **2018**, *4*, 199; d) L. Ackermann, *Chem. Rev.* **2011**, *111*, 1315.

[16] M. C. Whisler, S. MacNeil, V. Snieckus, P. Beak, *Angew. Chem. Int. Ed.* **2004**, *43*, 2206.

[17] a) N. Kuhl, M. N. Hopkinson, J. Wencel-Delord, F. Glorius, *Angew. Chem. Int. Ed.* **2012**, *51*, 10236; b) J. F. Hartwig, M. A. Larsen, *ACS Cent. Sci.* **2016**, *2*, 281.

[18] Ó. López, J. M. Padrón, *Catalysts* **2022**, *12*, 164.

[19] A. Mondal, M. van Gemmeren, *Angew. Chem. Int. Ed.* **2022**, *61*, e202210825.

[20] To aid the comparison of examples, a threshold of 5 mol% was used to indicate high catalyst loading, and a threshold of 100 °C was used to indicate high reaction temperature.

[21] a) D. A. Colby, R. G. Bergman, J. A. Ellman, *Chem. Rev.* **2010**, *110*, 624; b) S. Rej, N. Chatani, *Angew. Chem. Int. Ed.* **2019**, *58*, 8304.

[22] S. Dongbang, B. Pedersen, J. A. Ellman, *Chem. Sci.* **2019**, *10*, 535.

[23] T. Mesganaw, J. A. Ellman, *Org. Process Res. Dev.* **2014**, *18*, 1105.

[24] a) P. B. Arockiam, C. Bruneau, P. H. Dixneuf, *Chem. Rev.* **2012**, *112*, 5879; b) P. Nareddy, F. Jordan, M. Szostak, *ACS Catal.* **2017**, *7*, 5721.

[25] M. Seki, *ACS Catal.* **2011**, *1*, 607.

[26] M. Seki, M. Nagahama, *J. Org. Chem.* **2011**, *76*, 10198.

[27] A. Mehta, B. Saha, A. A. Koohang, M. S. Chorghade, *Org. Process Res. Dev.* **2018**, *22*, 1119.

[28] S. G. Ouellet, A. Roy, C. Molinaro, R. Angelaud, J. F. Marcoux, P. D. O'Shea, I. W. Davies, *J. Org. Chem.* **2011**, *76*, 1436.

[29] D. G. Johns, S.-P. Wang, R. Rosa, J. Hubert, S. Xu, Y. Chen, T. Bateman, R. O. Blaustein, *Pharmacol. Res. Perspect.* **2019**, *7*, e00543.

[30] M. Seki, *Synthesis* **2012**, *44*, 3231.

[31] M. Seki, *RSC Adv.* **2014**, *4*, 29131.

[32] M. Seki, *Synthesis* **2015**, *47*, 1423.

[33] M. Seki, *Synthesis* **2015**, *47*, 2985.

[34] For alternative synthetic routes to obtain candesartan cilexetil and olmesartan medoxomil, see: M. Seki, Y. Takahashi, *Synthesis* **2021**, *53*, 2689.

[35] a) J. H. B. I. A. I. Mkhalid, T. B. Marder, J. M. Murphy, J. F. Hartwig, *Chem. Rev.* **2010**, *110*, 890; b) J. S. Wright, P. J. H. Scott, P. G. Steel, *Angew. Chem. Int. Ed.* **2021**, *60*, 2796; c) C. Haldar, M. E. Hoque, J. Chaturvedi, M. M. M. Hassan, B. Chattopadhyay, *Chem. Commun.* **2021**, *57*, 13059.

[36] M. A. Larsen, J. F. Hartwig, *J. Am. Chem. Soc.* **2014**, *136*, 4287.

[37] E. A. Lim, J. C. Bendell, G. S. Falchook, T. M. Bauer, C. G. Drake, J. H. Choe, D. J. George, J. L. Karlix, S. Ulahannan, K. F. Sachsenmeier, D. L. Russell, G. Moorthy, B. S. Sidders, E. A. Pilling, H. Chen, M. M. Hattersley, M. Das, R. Kumar, G. P. Pouliot, M. R. Patel, *Clin. Cancer Res.* **2022**, *28*, 4871.

[38] J. J. Douglas, B. W. V. Adams, H. Benson, K. Broberg, P. M. Gillespie, O. Hoult, A. K. Ibraheem, S. Janbon, G. Janin, C. D. Parsons, R. C. Sigerson, D. J. Klauber, *Org. Process Res. Dev.* **2019**, *23*, 62.

[39] A. J. Lyons, A. Clarke, H. Fisk, B. Jackson, P. R. Moore, S. Oke, T. O. Ronson, R. E. Meadows, *Org. Process Res. Dev.* **2022**, *26*, 1378.

[40] K. Arrington, G. A. Barcan, N. A. Calandra, G. A. Erickson, L. Li, L. Liu, M. G. Nilson, I. Strambeanu, K. F. VanGelder, J. L. Woodard, S. Xie, C. L. Allen, J. A. Kowalski, D. C. Leitch, *J. Org. Chem.* **2019**, *84*, 4680.

[41] "*Complete Accounts of Integrated Drug Discovery and Development: Recent Examples from the Pharmaceutical Industry Volume 2*": A. J. Peat, S. Xie, *ACS Symposium Series*, *Vol. 1332*, American Chemical Society, Washington, **2019**, p. 297

[42] S. Karlsson, H. Benson, C. Cook, G. Currie, J. Dubiez, H. Emtenäs, J. Hawkins, R. Meadows, P. D. Smith, J. Varnes, *Org. Process Res. Dev.* **2022**, *26*, 601.

[43] S. M. Preshlock, D. L. Plattner, P. E. Maligres, S. W. Krska, R. E. Maleczka Jr, M. R. Smith III, *Angew. Chem. Int. Ed.* **2013**, *52*, 12915.

[44] R. N. Bream, H. Clark, D. Edney, A. Harsanyi, J. Hayler, A. Ironmonger, N. Mc Cleary, N. Phillips, C. Priestley, A. Roberts, P. Rushworth, P. Szeto, M. R. Webb, K. Wheelhouse, *Org. Process Res. Dev.* **2021**, *25*, 529.

[45] M. G. Matera, M. Cazzola, C. Page, *Curr. Opin. Pharmacol.* **2021**, *56*, 74.

[46] L.-C. Campeau, Q. Chen, D. Gauvreau, M. Girardin, K. Belyk, P. Maligres, G. Zhou, C. Gu, W. Zhang, L. Tan, P. D. O'Shea, *Org. Process Res. Dev.* **2016**, *20*, 1476.

[47] a) O. Daugulis, H.-Q. Do, D. Shabashov, *Acc. Chem. Res.* **2009**, *42*, 1074; b) X. Chen, K. M. Engle, D.-H. Wang, J.-Q. Yu, *Angew. Chem. Int. Ed.* **2009**, *48*, 5094; c) S. Kancherla, K. B. Jørgensen, M. Á. Fernández-Ibáñez, *Synthesis* **2019**, *51*, 643.

[48] L.-C. Campeau, S. Rousseaux, K. Fagnou, *J. Am. Chem. Soc.* **2005**, *127*, 18020.

[49] H. Zhao, R. Wang, P. Chen, B. T. Gregg, M. M. Hsia, W. Zhang, *Org. Lett.* **2012**, *14*, 1872.

[50] M. S. McClure, B. Glover, E. McSorley, A. Millar, M. H. Osterhout, F. Roschangar, *Org. Lett.* **2001**, *3*, 1677.

[51] a) G. Zeni, R. C. Larock, *Chem. Rev.* **2006**, *106*, 4644; b) L.-C. Campeau, M. Parisien, A. Jean, K. Fagnou, *J. Am. Chem. Soc.* **2006**, *128*, 581; c) T. Watanabe, S. Oishi, N. Fujii, H. Ohno, *J. Org. Chem.* **2009**, *74*, 4720; d) R. B. Bedford, M. Betham, *J. Org. Chem.* **2006**, *71*, 9403; e) S. I. Gorelsky, D. Lapointe, K. Fagnou, *J. Am. Chem. Soc.* **2008**, *130*, 10848.

[52] G. Erickson, J. Guo, M. McClure, M. Mitchell, M.-C. Salaun, A. Whitehead, *Tetrahedron Lett.* **2014**, *55*, 6007.

[53] J. J. Dong, J. Roger, F. Požgan, H. Doucet, *Green Chem.* **2009**, *11*, 1832.

[54] B. Liégault, D. Lapointe, L. Caron, A. Vlassova, K. Fagnou, *J. Org. Chem.* **2009**, *74*, 1826.

[55] a) H. Chen, M. Farizyan, F. Ghiringhelli, M. van Gemmeren, *Angew. Chem. Int. Ed.* **2020**, *59*, 12213; b) H. Chen, M. Farizyan, M. van Gemmeren, *Eur. J. Org. Chem.* **2020**, 6318; c) A. Mondal, M. van Gemmeren, *Angew. Chem. Int. Ed.* **2021**, *60*, 742.

[56] V. R. R. Ambati, Srinivas Garaga, Sambhu Prasad Sarma Mallela, S. Meenakshisunderam (A. P. Ltd.), WO2010095024 A2, **2010**.

[57] S. M. Gaulier, R. McKay, N. A. Swain, *Tetrahedron Lett.* **2011**, *52*, 6000.

[58] M. S. Chambers, S. C. Goodacre, D. J. Hallett, A. Jennings, P. Jones, R. T. Lewis, K. W. Moore, L. J. Street, H. J. Szekeres (MSD), WO02074772 A1, **2002**.

[59] M. S. Jensen, R. S. Hoerrner, W. Li, D. P. Nelson, G. J. Javadi, P. G. Dormer, D. Cai, R. D. Larsen, *J. Org. Chem.* **2005**, *70*, 6034.

[60] M. Cameron, B. S. Foster, J. E. Lynch, Y.-J. Shi, U.-H. Dolling, *Org. Process Res. Dev.* **2006**, *10*, 398.

[61] a) B. J. Kaminski, M. L. Van Linn, J. M. Cook, W. Yin, E. M. Weerts, *Psychopharmacology* **2013**, *227*, 127; b) A. F. Holtyn, V. V. N. P. B. Tiruveedhula, M. R. Stephen, J. M. Cook, E. M. Weerts, *Drug Alcohol Depend.* **2017**, *170*, 25.

[62] H. L. June, K. L. Foster, P. F. McKay, R. Seyoum, J. E. Woods, S. C. Harvey, W. J. A. Eiler, C. Grey, M. R. Carroll, S. McCane, C. M. Jones, W. Yin, D. Mason, R. Cummings, M.

© 2023 The Authors. Angewandte Chemie International Edition published by Wiley-VCH GmbH

15213773, 2023, 45, Downloaded from https://onlinelibrary.wiley.com/doi/10.1002/anie.202306659 by Christian-Albrechts-Universitat, Wiley Online Library on [22/01/2025]. See the Terms and Conditions (https://onlinelibrary.wiley.com/terms-and-conditions) on Wiley Online Library for rules of use; OA articles are governed by the applicable Creative Commons License

Garcia, C. Ma, P. V. V. S. Sarma, J. M. Cook, P. Skolnick, *Neuropsychopharmacology* **2003**, *28*, 2124.
[63] O. A. Namjoshi, A. Gryboski, G. O. Fonseca, M. L. Van Linn, Z. J. Wang, J. R. Deschamps, J. M. Cook, *J. Org. Chem.* **2011**, *76*, 4721.
[64] V. V. N. Phani Babu Tiruveedhula, K. R. Methuku, J. R. Deschamps, J. M. Cook, *Org. Biomol. Chem.* **2015**, *13*, 10705.
[65] S. R. Wisniewski, J. M. Stevens, M. Yu, K. J. Fraunhoffer, E. O. Romero, S. A. Savage, *J. Org. Chem.* **2019**, *84*, 4704.
[66] S. R. Wisniewski, S. A. Savage, E. O. Romero, M. D. Eastgate, Y. Tan, E. M. Simmons, R. E. Plata, J. R. Sowa Jr., D. G. Blackmond, *J. Org. Chem.* **2019**, *84*, 7961.
[67] H. Zhang, B. X. Li, B. Wong, A. Stumpf, C. G. Sowell, F. Gosselin, *J. Org. Chem.* **2019**, *84*, 4796.
[68] W. J. Omeljaniuk, R. Krętowski, W. Ratajczak-Wrona, E. Jabłońska, M. Cechowska-Pasko, *Int. J. Mol. Sci.* **2021**, *22*, 11511.
[69] J. Berdeja, F. Palandri, M. R. Baer, D. Quick, J. J. Kiladjian, G. Martinelli, A. Verma, O. Hamid, R. Walgren, C. Pitou, P. L. Li, A. T. Gerds, *Leuk. Res.* **2018**, *71*, 82.
[70] D. Mitchell, K. P. Cole, P. M. Pollock, D. M. Coppert, T. P. Burkholder, J. R. Clayton, *Org. Process Res. Dev.* **2012**, *16*, 70.
[71] A. N. Campbell, K. P. Cole, J. R. Martinelli, S. A. May, D. Mitchell, P. M. Pollock, K. A. Sullivan, *Org. Process Res. Dev.* **2013**, *17*, 273.
[72] D. Lapointe, K. Fagnou, *Org. Lett.* **2009**, *11*, 4160.
[73] J. Aziz, S. Piguel, *Synthesis* **2017**, *49*, 4562.
[74] K. Kuroda, S. Tsuyumine, T. Kodama, *Org. Process Res. Dev.* **2016**, *20*, 1053.
[75] S. Pivsa-Art, T. Satoh, Y. Kawamura, M. Miura, M. Nomura, *Bull. Chem. Soc. Jpn.* **1998**, *71*, 467.
[76] J. Huang, J. Chan, Y. Chen, C. J. Borths, K. D. Baucom, R. D. Larsen, M. M. Faul, *J. Am. Chem. Soc.* **2010**, *132*, 3674.
[77] S. Caille, S. Cui, M. M. Faul, S. M. Mennen, J. S. Tedrow, S. D. Walker, *J. Org. Chem.* **2019**, *84*, 4583.
[78] V. J. Cee, M. Frohn, B. A. Lanman, J. Golden, K. Muller, S. Neira, A. Pickrell, H. Arnett, J. Buys, A. Gore, M. Fiorino, M. Horner, A. Itano, M. R. Lee, M. McElvain, S. Middleton, M. Schrag, D. Rivenzon-Segal, H. M. Vargas, H. Xu, Y. Xu, X. Zhang, J. Siu, M. Wong, R. W. Burli, *ACS Med. Chem. Lett.* **2011**, *2*, 107.
[79] J. Yin, D. Zhan, H. Ma, H. Liu, L. Yu, Y. Zhang, F. Nan, *Org. Process Res. Dev.* **2021**, *25*, 2260.
[80] A. Pinto, L. Neuville, P. Retailleau, J. Zhu, *Org. Lett.* **2006**, *8*, 4927.
[81] a) K. Gilmore, I. V. Alabugin, *Chem. Rev.* **2011**, *111*, 6513; b) J. E. Baldwin, *J. Chem. Soc. Chem. Commun.* **1976**, 734.
[82] E. J. Hennessy, S. L. Buchwald, *J. Am. Chem. Soc.* **2003**, *125*, 12084.
[83] M. R. Barbachyn, D. K. Hutchinson, S. J. Brickner, M. H. Cynamon, J. O. Kilburn, S. P. Klemens, S. E. Glickman, K. C. Grega, S. K. Hendges, D. S. Toops, C. W. Ford, G. E. Zurenko, *J. Med. Chem.* **1996**, *39*, 680.
[84] T. W. Waldrep, D. J. Skiest, *Pharmacotherapy* **2002**, *22*, 109.
[85] A. Choy, N. Colbry, C. Huber, M. Pamment, J. V. Duine, *Org. Process Res. Dev.* **2008**, *12*, 884.
[86] W. P. Castelli, R. J. Garrison, P. W. F. Wilson, R. D. Abbott, S. Kalousdian, W. B. Kannel, *JAMA J. Am. Med. Assoc.* **1986**, *256*, 2835.
[87] R. Hutchings, W. Park, G. Bolton, C. Van Huis, J. Kohrt (Pfizer), US20080287479 A1, **2008**.
[88] E. J. Kiser, J. Magano, R. J. Shine, M. H. Chen, *Org. Process Res. Dev.* **2012**, *16*, 255.
[89] G. S. Tria, T. Abrams, J. Baird, H. E. Burks, B. Firestone, L. A. Gaither, L. G. Hamann, G. He, C. A. Kirby, S. Kim, F. Lombardo, K. J. Macchi, D. P. McDonnell, Y. Mishina, J. D. Norris, J. Nunez, C. Springer, Y. Sun, N. M. Thomsen, C. Wang, J. Wang, B. Yu, C.-L. Tiong-Yip, S. Peukert, *J. Med. Chem.* **2018**, *61*, 2837.
[90] M. Baenziger, M. Baierl, K. Devanathan, S. Eswaran, P. Fu, B. Gschwend, M. Haller, G. Kasinathan, N. Kovacic, A. Langlois, Y. Li, F. Schuerch, X. Shen, Y. Wan, R. Wickendick, S. Xie, K. Zhang, *Org. Process Res. Dev.* **2020**, *24*, 1405.
[91] J. Bien, A. Davulcu, A. J. DelMonte, K. J. Fraunhoffer, Z. Gao, C. Hang, Y. Hsiao, W. Hu, K. Katipally, A. Littke, A. Pedro, Y. Qiu, M. Sandoval, R. Schild, M. Soltani, A. Tedesco, D. Vanyo, P. Vemishetti, R. E. Waltermire, *Org. Process Res. Dev.* **2018**, *22*, 1393.
[92] A. P. Kozikowski, D. Ma, *Tetrahedron Lett.* **1991**, *32*, 3317.
[93] A. V. Purandare, T. M. McDevitt, H. Wan, D. You, B. Penhallow, X. Han, R. Vuppugalla, Y. Zhang, S. U. Ruepp, G. L. Trainor, L. Lombardo, D. Pedicord, M. M. Gottardis, P. Ross-Macdonald, H. de Silva, J. Hosbach, S. L. Emanuel, Y. Blat, E. Fitzpatrick, T. L. Taylor, K. W. McIntyre, E. Michaud, C. Mulligan, F. Y. Lee, A. Woolfson, T. L. Lasho, A. Pardanani, A. Tefferi, M. V. Lorenzi, *Leukemia* **2012**, *26*, 280.
[94] M. A. Fitzgerald, O. Soltani, C. Wei, D. Skliar, B. Zheng, J. Li, J. Albrecht, M. Schmidt, M. Mahoney, R. J. Fox, K. Tran, K. Zhu, M. D. Eastgate, *J. Org. Chem.* **2015**, *80*, 6001.
[95] R. J. Fox, N. L. Cuniere, L. Bakrania, C. Wei, N. A. Strotman, M. Hay, D. Fanfair, C. Regens, G. L. Beutner, M. Lawler, P. Lobben, M. C. Soumeillant, B. Cohen, K. Zhu, D. Skliar, T. Rosner, C. E. Markwalter, Y. Hsiao, K. Tran, M. D. Eastgate, *J. Org. Chem.* **2019**, *84*, 4661.
[96] Y. Ji, R. E. Plata, C. S. Regens, M. Hay, M. Schmidt, T. Razler, Y. Qiu, P. Geng, Y. Hsiao, T. Rosner, M. D. Eastgate, D. G. Blackmond, *J. Am. Chem. Soc.* **2015**, *137*, 13272.

Manuscript received: May 11, 2023
Accepted manuscript online: June 7, 2023
Version of record online: August 9, 2023

© 2023 The Authors. Angewandte Chemie International Edition published by Wiley-VCH GmbH

15213773, 2023, 45, Downloaded from https://onlinelibrary.wiley.com/doi/10.1002/anie.202306659 by Christian-Albrechts-Universitat, Wiley Online Library on [22/01/2025]. See the Terms and Conditions (https://onlinelibrary.wiley.com/terms-and-conditions) on Wiley Online Library for rules of use; OA articles are governed by the applicable Creative Commons License